התקן זרימה במיקרו-תעלות לחקר זרימת הדם במיקרוצירקולציה

ראיד חמאיסי

התקן זרימה במיקרו-תעלות לחקר זרימת הדם במיקרוצירקולציה

חיבור על עבודת גמר

לשם מילוי חלקי של הדרישות לקבלת התואר

מגיסטר למדעים בהנדסה ביו-רפואית

ראיד חמאיסי

הוגש לסנט הטכניון –מכון טכנולוגי לישראל

אדר תשס"ו חיפה פברואר 2006

עבודת הגמר נעשתה בהנחיית פרופ' אורי דינר* ופרופ' יעל נמירובסקי** בפקולטה להנדסה ביו-רפואית.
ברצוני להודות לפרופסור אורי דינר ולפרופסור יעל נמירובסקי על הנחייתם המסורה. זה היה כבוד גדול , הן בהיבט האישי והן בהיבט המקצועי לעבוד תחת הנחייתם.

אני מודה להורי , למשפחתי ולאשתי על תמיכתם לאורך כל הדרך.

אני מודה לטכניון על התמיכה הכספית הנדיבה בהשתלמותי.

* הפקולטה להנדסה ביו-רפואית - טכניון

** הפקולטה להנדסה חשמל - טכניון

תוכן עניינים

תוכן עניינים (המשך)

רשימת איורים

רשימת איורים (המשך)

רשימת טבלות

תקציר

היום ישנה התעניניות גוברת במחקר של זרימה במיקרו-מערכות, כאשר ישנם הרבה תחומים שזקוקים לתחום המחקר החדשני הזה למשל (מכניקה- של תורת הזרימה,מערכות אנליזה כימיות ומערכות מינון זעירות) .קיימים מחקרים רבים של מיכניקת תורת הזרימה ברמה המיקרונית במיוחד חקירת הזרימה בגוף האדם ומערכת המיקרו-צירקולציה בפרט, מערכות אנליזה כימיות ובילוגיות .

מיקרו-מערכות זרימה לוקחות תפקיד ראשי בפיתוח הרבה פעילויות מחקריות חדישות, כאשר שואפים בעזרתן לפיתוח התקנים ומערכות זעירות.אחד המרכיבים הבסיסים של מיקרו-מערכות זרימה הוא מיקרו-תעלות.

בעשור האחרון ישנם מחקרים מעניינים במיקרו-מערכות זרימה, בפיתוח מיקרו-מערכות לתחום הרפואה או הביולוגיה יש עניין מחקרי של זרימת במיקרו-תעלות.

ישנם הרבה אפליקציות רפואיות ובילוגיות של מיקרו-מערכות זרימה כמו מנופולציה וממיינים של תאים , מערכות אבחון, הסתעפות של מיקרו-תעלות תוכל לשמש אנלוג מעבדתי של רשת הנימים בתוך מערכת המיקרו-צירקולציה. לבנות מערכות אלו נדרשת הבנה איך נוזלים בילוגים זורמים ומתנהגים במיקרו מבנים.

חשיבות מערכת המיקרו-צירקולציה מודגשת בעובדה שרוב ההתנגדות ההידרודינמית של מערכת הצירקולציה נמצאת באזור רשת הנימים.

מטרת המחקר הנה להבין יותר טוב את זרימת הדם במיקרו-צירקולציה ,לימידת הפרמטרים הבילוגים שלה הנדרשים לחקירה ברמה המקרונית וחיזוי של התנהגות הזרימה. לכן אחד העיקרים בהתעניונות בתוך מערכת המיקרו-צירקולציה מיכיל את קצב הזרימה כפונקציה של הפרש הלחצים בתוכה.

מטרה נוספת של החקירה השוואת התנהגות הזרימה של נוזלים בילוגיים שונים במיקרו-תעלות עם מים מזוקקים, נבחן התנהגות של מים מזוקקים, אתנול, איזופרופנול וגליצרין.והאחרונה היא להראות את היכולות של טכניקת הייצור של מיקרו –מערכות לתחום זה.

להשגת מטרה זו, החקר נעשה בשני משורים: ייצור של מודול מעבדתי ,ובמישור הניסויי.

במישור הראשון פותח וייוצר מודול מעבדתי, כאשר לקח בחשבון את את רוב האמפינים המביניים והגיאומטרים של מערכת המיקרו-צירקולציה, כך שאפשר לחקור את הפרמטרים של מערכת המיקרו-צירקולציה. הרכיב העקרי של המודול הן מיקרו-תעלות.

המודול ייוצר בשיטות פוטוליטוגרפיה, על שבב סיליקון בעובי של 300 מיקרון. המודול מכיל שלוש טופולוגיות של מיקרו-תעלות אשר לכל אחת יש חשבות בתוך המיקרו-צירקולציה. על מנת ללמוד את השפעת גודל כלי הדם על הזרימה, תוכננו מיקרו-תעלות עם גדלים שונים. הגדולה מתוכן יכולה לדמות ארטריולה עם קוטר בערך 50 מיקרון,לחלופים הקטנה מתוכן יכולה לדמות נימים עם קוטר בערך 10 מיקרון. תוכננו מיקרו-תעלות מפוצלות לספק מודל של זרימת דם בנקודת התפצלות מכלי דם גדול לכלי דם יותר קטנים.

חלק מן המודים שתוכננו לניסויי:

- מיקרו-תעלות ישרות באורך של 11מ"מ בעלי קוטר הידראולי של 15- 60 מיקרון,למיקרו-תעלות יש חתכים שונים (חתך משולשי, חתך טרפזי וחתך חצי מעגלי).
- מיקרו-תעלות בצורת לולאה ,כאשר ישנם שני מודולים אחד עם שתי לולאות והשני עם שלוש לולאות , למיקרו-תעלות יש חתך חצי מעגלי בעל קוטר הידראולי של 48.8 מיקרון.
- מיקרו-תעלות שעוברות פיצול לשתי מיקרו-תעלות אחרות עם קוטר הידראולי שונה, עם חתכים שונים.

לבסוף חוברה פיסת פיירקס, בהדבקה אנודית, לצד המיקרו-תעלות כדי לייצור מיקרו-תעלות סגורות ואטומות ורק ישנם פתחי כניסה ויציאה בלבד.

במישור הניסויי נבנתה מערכת ניסויי המאפשרת למדוד את קצב הזרימה כפונקציה של הפרש הלחצים על המיקרו-תעלה. השתמשנו במערכת במודולים השונים

התוצאות הראו שהשימוש בטכניקת הייצור של מיקרו –מערכות לתחום זה יעילה מאוד, ייצור המיקרו-תעלות על פיסת סיליקון קשיחה מאפשר שליטה טובה מאוד לייצור רשת של מיקרו-תעלות בכדי ללמוד את מערכת המיקרו-צירקולציה.

תוצאות המחקר הראו שהזרימה במיקרו-תעלות מתנהגת בדומה להתנהגותה בתעלות בגדלים רגלים, השיטות הרגילות שהשתמשנו לעריכת הניסויים הינן מספיקות.

נמצאה התנהגות ליניארת של קצב הזרימה כפונקציה של הפרש הלחצים על המיקרו-תעלה בכל הניסויים כמו במודלים התיאורטים ,כמו כן התנהגות זו קיימת בזרימה למינארת רגילה . בגדלים שונים של קוטר הידראולי לא נמצאו התנגדות שונות אפילו בגלים קטים של 15 מיקרון.אין השפעה לסוג החתך של המיקרו-תעלה על קצב הזרימה כפונקציה של הפרש הלחצים.

הזרימה במיקרו-תעלות מטבעה עם מספרי רינולדס קטנים,לפי ניסויים בגדלים שונים של מיקרו-תעלות (שטח חתך) מצאנו השפעה גדולה מאוד של שטח החתך על מספרי רינולדס כך כאשר תעלה גדלה אשר מיוצגת בקוטר הידראולי גדול מספר רינולדס גדל.

הצלחנו לבצע את הנסויים והחקירה עבור הנוזלים הבאים : מים מזוקקים, אתנול, איזופרופנול וגליצרין ,לפי ההשוואה שביצענו מצאנו התנהגות ליניארת של קצב הזרימה כפונקציה של הפרש הלחצים ,דומה לזו של זרימה למינארת רגילה.

לסיכום ניתן לומר כי מחקר זה מתאר היטב את הזרימה במיקרו-תעלות וממפה סוגים שונים של מיקרו-תעלות.

הבנת הזרימה מאפשרת לפתח ולבנות מיקרו-מערכות לאפליקציות רפואיות ובילוגיות .

אפשר להרחיב את השימוש של מערכת זו לאפליקציות נוספות, המערכת יכולה לספק תצפית לתגובות התאים לשכבת תאי אינדותל אשר אפשר לצפות את המיקרו-תעלות. המערכת מאפשרת לצפות בזרימה של תאי הדם בתוך

רשת מיקרו-תעלות דומה לזו הקיימת במערכת המיקרו-צירקולציה.

מערכת חדשנית זו יכולה לשמש כבסיס להמון מחקרים ובתחומים נוספים, מנופולציה ומיון תאים ,אמצעים לאבחון, כמו כן מיקרו-תעלות מפוצלות יכולות להיות בסיס לבנית רשת כפילרות מעבדתית.

MICROCHANNEL FLOW DEVICE FOR THE STUDY OF MICROCIRCULATORY BLOOD FLOW

RAED KHAMAISI

MICROCHANNEL FLOW DEVICE FOR THE STUDY OF MICROCIRCULATORY BLOOD FLOW

FINAL PAPER

SUBMITTED IN PARTIAL FULFILLMENT OF THE REQUIREMENTS
FOR THE DEGREE OF MASTER OF SCIENCE
IN BIO-MEDICAL ENGINEERING

RAED KHAMAISI

Submitted to the Senate of the Technion –Israel Institute of Technology
ADAR, 5766 HAIFA FABRUARY 2006

THE FINAL PAPER WAS DONE UNDER THE SUPERVISION OF PROF. Uri Dinnar* AND PROF. Yael Namirovsky**, IN THE FACULTY OF BIO-MEDECAL ENGINEERING.

ACKNOWLEDGMENT

I wish to express my deep gratitude to my advisors, Professor Uri Dinnar* and Professor Yael Namirovsky** for their help and support.

I also wish to express deep gratitude to my parents, family and my wife for their unconditional support.

THE GENEROUS FINANCIAL HELP OF TECHNION IS GRATEFULLY ACKNOWLEDGED

*** Department of Biomedical Engineering, Technion**

**** Faculty of Electrical Engineering, Technion**

Table of Contents

List of Figures

List of Tables

Abstract

Today there is growing interest in research on microfluidic systems. (e.g., for rheological studies, chemical analysis systems and microdosage systems). Microfluidics plays a major role in the development of many innovative research activities aimed at developing miniaturized devices and systems. One of the basic components in microfluidic systems is microchannels.

In the last decade there is an interest in research on Microfluidics devices.

Development of medical or chemical micro-assembly system research concerns blood flow in microchannels.

There are many medical and biological applications for Microfluidics devices such as cell manipulation, sorters and diagnostic instruments. Branching microchannels may also serve as a laboratory analog for complex capillary networks in the blood circulatory system. To build these devices it is necessary to have an understanding of how the complex biological fluids behave inside small structures. The importance of the microcirculation is highlighted by the fact that most of the hydrodynamic resistance of the circulatory system lies in the microvessels.

The research goal is to better understand the Microcirculatory blood flow and the study of biomedical parameters of Microcirculatory. These parameters are needed to investigate the micro-level and to predict the flow behavior. The main interest in microcirculation includes pressure-flow relationship.

Another goal of this investigation is to compare the flow behavior of different biological fluids in microchannels with the behavior of Distilled water. We will examine the behavior of Distilled water, Isopropanol, Ethanol and Glycerin. And the last is to demonstrate the capabilities of the proposed microfabrication technique.

To achieve this goal, the research was conducted in two levels: fabrication of Lap-Biochip and experimental.

In the first part of our research we developed and fabricated a Lap-Biochip. This Lap-Biochip accounted for the most essential microstructural and geometrical features of Microcirculatory. This enabled the possibility of using Lap-Biochip to investigate the Microcirculatory parameters. The main component, which the Lap-Biochip builds around, is the microchannel.

The Lap-Biochip based microchannel was designed and fabricated by using standard planar photolithography process on a 300μm silicon substrate. It consists of three types of microchannel topologies, the first, are straight microchannels, 11mm long, having hydraulic diameters ranging

from 15μm to 60μm. These microchannels have different cross-sections, triangular, trapezoid and semi-circular shaped.

The second are looped microchannels having two modules with differences in the number of loops, two loops and three loops. These looped microchannels have semi-circular cross-sections with 48.8μm hydraulic diameter. The last, commonly encountered in microvessels, will enable the study of branching of, bifurcated microchannels.

The microchannels were sealed to a 7400 Pyrex substrate by anodic bonding to form the chip test module.

In the experimental part of this work, an apparatus was constructed and a procedure devised to measure the volume flow rate Q and the pressure drop across the microchannel ΔP. The test modules used straight microchannels, bifurcation microchannels and looped microchannels to study the differences in behaviors of blood and biological fluids.

The results indicated that the fabrication of the microchannel into rigid silicon offered excellent control for studying microcirculation on network microchannels.

The experimental result shows that the flow in microchannels behaves similar to the conventional size channels and the regular method used to evaluate the flow is satisfactory. The theoretical curves of the flow rate, as a function of the pressure drop, are all linear. The experimental curves of the flow rate were also linear, as required by conventional laminar flow theory.

The comparison of the flow of various fluids Isopropanol, Ethanol and Glycerin with Distilled water in straight microchannels behaved linear as expected in conventional laminar flow.

In summary it can be said that the present research proves that the flow maps several types of microchannels.

Understanding the flow makes it possible to develop and build Microfluidic devices for medical and biological applications.

This system could extend to other application. First the system can provide observation of cellular response to the endothelial lining of a vessel. Second, the system allows observation of blood cell flow through an extensive network of microvessels similar to those found in the microcirculation.

List of Symbols

A cross section area of the microchannel

P perimeter of the microchannel

L channel length

Re Reynolds number

f friction factor

k loss coefficient

U mean velocity

C friction factor constant ($C=f.\ Re$)

D_h hydraulic diameter of the microchannel

Re Reynolds number

ΔP pressure drop across the microchannel

$\frac{dp}{dx}$ pressure gradient

Q flow rate

Greek symbols

μ *Fluid dynamic viscosity*

ρ *Fluid density*

1 Introduction

1.1 Overview and Application

Over the past decade, micromachining technology has been used to develop a number of microfluidic systems in silicon, glass, quartz, and plastics. Microchannels and chambers are essential component of any such system. In addition to connecting different devices, microchannels are also used for reactant.

The research covers blood flow in microchannels.
There are many medical and biological applications for micro-devices such as cell manipulation, sorters and diagnostic instruments. Branching microchannels may also serve as a laboratory analog of complex capillary networks in the blood circulatory system.
To build these devices it is necessary to have an understanding of how the complex biological fluids behave inside small structures.

1.2 Research Motivation and Goals

Development of micro fluidic devices and systems is predicted to have a dramatic impact on the chemistry and life sciences. Plethora of already existing and under development microfluidic solutions, and the ever-increasing demand for the new ones, underlines their growing significance. Manipulation of low volumes of liquids offers unprecedented advantages including better flow and reaction control; low cost and faster time response over conventional systems.

Transport of a liquid within a particular microfluidic system is usually accomplished through a network of capillaries of several to several hundred-micron sizes. Thus, the understanding of the liquid flow through such capillaries is of paramount importance from the design and fabrication point of view of such systems.

The objectives of my research are:

- Develop and fabricate a Lap-Biochip including microchannels, which – accounts for the most essential microstructural and geometrical features of Microcirculatory.
- Using the Lap-Biochip to investigate the Microcirculatory parameters.
- Develop and fabricate experimental methodology to investigate Microfluidics.
- Visualize the flow inside the Lap-Biochip.
- Comparing various biological fluids.

2 Background and Literature Review

Several researchers have studied fluid flow in microchannels and found good agreement with the Navier-Stokes equations. The major researches done with Newtonian fluids and check several flow parameters and fluid characteristics, the researches done in two planes experimentally and theoretically.

So far, relatively little has been known about the Non-Newtonian liquids flow and biological fluids, even less about the most important one - blood. Understanding of blood flow in microchannels is important from the medical point of view as well as from the viewpoint of the design and fabrication of future blood microanalysis systems.

2.1 Experimental Observations

In recent studies, Papautsky et al. [12] examined flow of water through arrays of surface micromachined metallic microchannels on top of silicon substrates. These channels had rectangular cross-section with inner width ranging from 150 μm to 600 μm and inner heights varying from 22.71 μm to 26.35 μm. Liquid input ports were etched through the silicon substrate. Additional ports were etched through silicon for static pressure measurements approximately 4.5 mm downstream, which eliminated entrance effects. The open ends of the microchannels extending off the silicon substrate were used as flow outlets. The channel length between the static pressure port and the open end was 7.75 mm. The channel cross-sectional dimensions were measured with a surface profilometer with a precision of 10 nm. Surface roughness of the microchannels was determined to be approximately 0.00033 using atomic force microscopy. The liquid flow was supplied by a controllable syringe pump. The uncertainty analysis showed the average uncertainties in f and Re to be 7.77% and 1.51% respectively at low pressures and 5.61% and 0.13% at high pressures. The experimental data of this study, are for $0.001 < Re < 10$ and shows a 20% increase in the normalized friction constant $(C^* \approx 1.2)$ from the theoretical values.

Similar results were obtained by Jiang et al. [19], who investigated flow of water through microchannels, nozzles, and diffusers. Microchannels used in this study had rectangular, trapezoidal, or triangular cross-sections, and were formed by KOH etching a silicon substrate then sealed by bonding it with a glass wafer. The microchannel dimensions ranged from 35 μm to 110

μm in width and from 13.4 μm to 46 μm in height, whereas the lengths varied from 2.5 mm to 10 mm. The authors did not specify roughness of the channel surfaces. Pressure measurements were taken using external pressure transducers, while volumetric flow rates were derived from observations of meniscus position using a microscope and a CCD camera. For the 10 mm long microchannel, *Re* ranged from 0.1 to 10 and the normalized friction constant is 15-30% above the theoretical values ($1.15 < C^* < 1.3$). For the shorter 5 mm channel with the identical cross-sectional dimensions, the flow data are in the same *Re* range but have a significantly higher normalized friction constant ($1.5 < C^* < 1.75$). Since channel length is the only difference between the two cases, the increase in the normalized friction constant might be attributed to the entrance effects in the shorter channels.

Gale [20] investigated flow of water through individual microchannels of low aspect ratio. The microchannels fabricated as a part of a biochemical analysis system were formed using an epoxy-like polymer sandwiched between a bottom silicon substrate and a top glass cover. The channel widths ranged from 4 mm to 6 mm while heights varied from 14.5 μm to 50 μm. The channel input ports were etched through the silicon substrates. Additional ports were etched in silicon for static pressure measurements 4.5 mm downstream in order to eliminate entrance and exit effects. The channel length between the static pressure ports was 5 mm. The channel height measurements were performed using a microscope with z-dimension measurement capability with resolution of 1 μm. Roughness of the microchannel inner surface was not characterized. A controllable syringe pump supplied the liquid flow. The data collected in this study are for $0.1 < Re < 20$. The data appear within ±30% of the theoretical values ($0.7 < C^* < 1.35$). The author suggested that such a large variation in the normalized friction constant is due to variation in channel height along the channel length. It is also possible that wide range in the normalized friction constant is due to the poor measurement of the microchannel height.

Wilding et al. [8] analyzed flow of water and various biological fluids (saline, serum, plasma, and whole blood) in glass-capped silicon microchannels. The channels had trapezoidal cross-section with dimensions of 80x20 μm2 (WxH) and 150x40 μm2. Entrance and exit ports (500x500 μm2) were etched through the silicon substrate with spacing (i.e. channel length) of 11. 7 mm. The channel dimensions were measured with a surface profilometer with a precision of ±1 %. The authors did not specify roughness of the microchannels. The liquid flow was supplied by

connecting the inlet port to a syringe whose plunger was actuated by a stepper motor. A load cell measured the applied force from which the driving pressure was deduced. The force measurement was corrected for frictional losses in the system. The authors estimated the pressure losses in the syringe and supply piping to be less than 1 % of the total pressure drop. The experimental data of this study are for $10 < Re < 100$ and indicate a 30% increase in the normalized friction constant ($C^* \approx 1.3$) from the theoretical values.

Pfhaler et al [4,5], Weilin et al [7] and Papautsky et al [12] assumed the deviation would originate from surface phenomena such as surface roughness, electrokinetic forces, temperature effects and microcirculation near the wall. Most results indicate that the friction factor/pressure gradient would increase due to effects of surface phenomena.

G. Hetsroni [22], in recent literature review considering the problem of liquid flow in microchannels under conditions of small Reynolds numbers that correspond to continuum model. Data from the literature on pressure drop in circular, rectangle, triangular and trapezoidal micro-channels with hydrodynamic diameter ranging from 15 μm to 4010 μm are analyzed. The comparison of experimental results to those obtained by conventional theory is correct when the experimental conditions were consistent with the theoretical ones. The experimental results corresponding to these requirements agree quite well with the theory. The behavior of fluid flow in smooth microchannels of hydraulic diameter from 15 to 4010 μm, in the range of Reynolds number $Re < Recr$ the Poiseuille number,
Po is independent of the Reynolds number, Re. The behavior of the flow in microchannels, at least down to 50 μm diameter, shows no differences with macro-scale flow. The relation of hydraulic diameter to channel length and the Reynolds number are important factors that determine the effect of the viscous energy dissipation on flow parameters.

2.2 Using Microchannels for Understanding Blood Rheology

Kikuchi el al [21], using silicon device including 2600 microgrooves in parallel array for studies of blood Rheology and to examined blood erythrocyte deformability, the microgrooves as blood flow channels in single-crystal silicon is described. Grooves were formed in the (100) crystalline surface by means of photolithography and orientation-dependent etching. This substrate surface was tightly covered with an optically flat glass plate to prevent leakage. This structure was used to microscopically observe flow behavior of blood cells. As a first design of such a cell-flow apparatus, many parallel same-size channels of relatively short length (equivalent diameter 6 microns, length 14.4 microns, number 2600) have been produced to simultaneously measure the total volume flow rate of blood under constant suction. Despite differences in cross-sectional shape and length, the ratio of blood flow velocity to pressure gradient in the channels was comparable with estimates for capillary vessels in vivo. Activated white blood cells blocked the channels, while aggregations of red blood cells showed unexpectedly small resistance to channel transit.

Cokelet et al [15], develop a Microvascular flow system with circular cross sections by etching glass plates with mirror images of the vascular pattern.

David Trebotich and Wesley Chang et al. [16,17], investigated the use of simple power law model blood flow of between 2.5 and 100 μl/min in microchannels with 200 x 60 μm cross-sections and the following configuration: straight, 90 degree bend and a 2 to 1 sudden contraction in one transverse direction from 200 to 100μm, the specific objective of the study was to compare the measurements of pressure drop vs. flow rate for the blood flow in these microchannels with the calculations and found a consistent in the predictions of the magnitude of hydrodynamic resistances of the microchannels.

2.3 Newtonian Vs. Non-Newtonian fluids

The viscosity is the most important characteristic, which influences fluid-mechanical behavior, and relates to the local stresses in moving fluid to the strain rate of the fluid element.

When a fluid is sheared, it begins to move at a strain rate inversely proportional to a property called its *Coefficient of viscosity* μ [kg/(m.s)] or [cP], in fluids that this relationship is linear are called *Newtonian fluids.*

Fluids, which do not follow the linear relationship, are called *Non-Newtonian fluids.*

The viscosity varies with strong effect by temperature and moderate effect by pressure.

2.4 Blood Flow in Microvessels

Microvascular network is supplied with blood at a given driving pressure; the total blood flow and the distribution of the flow within the network are determined by its architecture and by the flow behavior of blood within it.

To understand the dynamics of the blood flow in Microvascular networks, it is necessary to consider first the composition of blood and its rheological behavior in narrow tubes and in their branch points, to be closer dimensionally to Microvascular networks using microchannels.

2.4.1 Blood

Blood is not a homogeneous fluid, is a viscous fluid mixture consisting of plasma and cells; Figure 1 illustrated the Components of Blood.

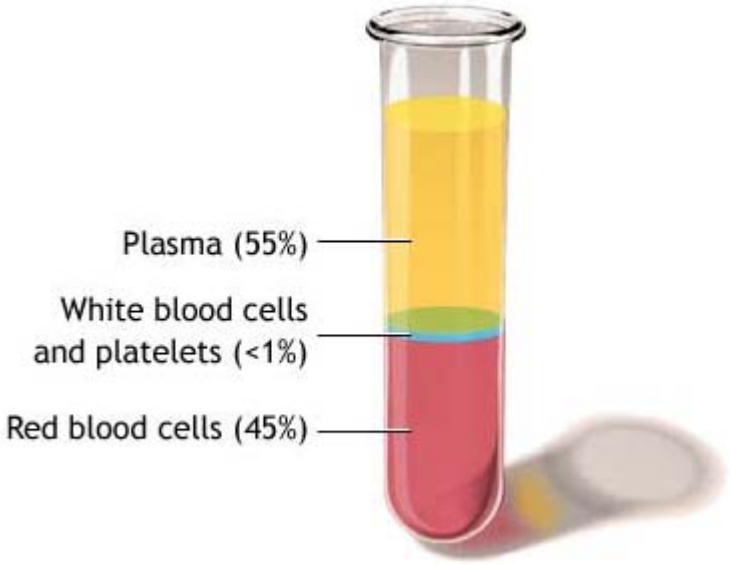

Figure 1: The Components of Blood [wab-1]

The human blood capacity is almost 5 liters, with 3 liters of the blood volume consisting of plasma (makes up about 55%). Blood plasma, itself considered the liquid matrix of blood, is a solution of proteins, electrolytes and other substances, which is nearly Newtonian fluid, and the remaining 2 liters represents the volume of the cellular component. The cellular component of blood consists of three main suspended cells types: Red blood cells (RBCs) Erythrocytes, White blood cells (WBCs) Leukocytes of several different types and Platelets. The blood flow properties are strongly influenced by the cells it contains in its suspension .The normal human blood has a

Hematocrit (volume fraction of red cells) of 45%, so the red cells strongly influence blood's flow properties. Blood cell dimensions are comparable to microvessels diameters, and continuum description of blood 's rheological properties, while appropriate for large vessels, is not adequate to describe blood flow in microvessels, The blood behavior in vessels smaller than approximately 100μm diameter exhibits significant non- Newtonian effects; flow in larger vessels can be described reasonably accurately using the Newtonian assumption.

Rheological properties of blood in arterioles and venules and larger vessels are determined primarily by (RBCs) Erythrocytes; however, (WBCs) Leukocytes play an important mechanical role in capillaries and small venules.

2.4.2 Viscosity of Blood

Blood plasma behaves like a Newtonian fluid with a coefficient of viscosity of about 1.2 cP. [24] However, whole blood (which includes red blood cells) is a non-Newtonian fluid. The blood plasma alone is incompressible but the addition of cellular components gives blood its non-Newtonian characteristics.

In whole blood, the viscosity varies with the hematocrit, the temperature and disease state, a non - Newtonian effect. Figure 2 illustrates the variation in the viscosity with shear rate and hematocrit. For a hematocrit of about 45%, the viscosity varies between 10 and 100 cP.

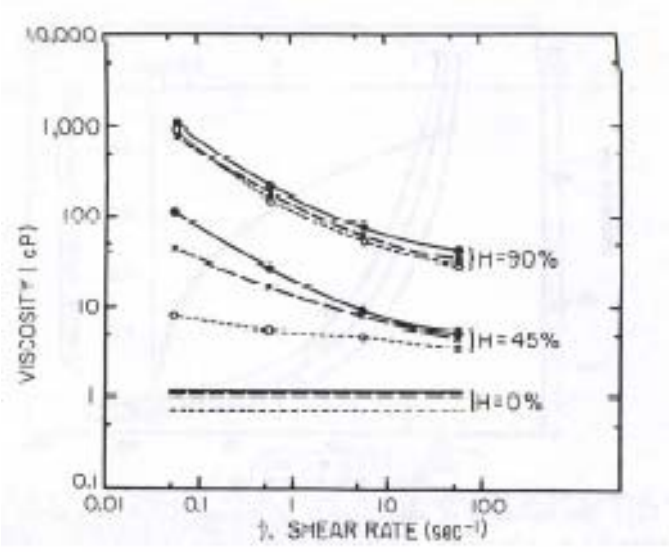

Figure 2: Variation of viscosity of whole blood with shear rate and hematocrit [24]

The main mechanism of the non-Newtonian behavior is RBC aggregation and the secondary mechanism is RBC deformation under shear force.

- Erythrocytes (RBCs)

The most abundant cells in the cellular component are the red blood cells (RBCs) or Erythrocytes Figure 3, comprising about 40-50% of the cellular component of the blood.

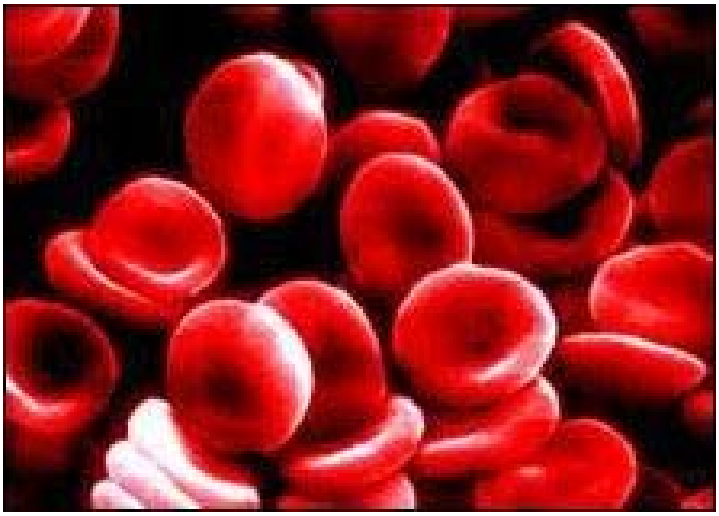

Figure 3: Red Blood Cells [wab-2]

The chief function of the RBCs is the delivery of O2 to tissue. RBCs are so easily deformable; as long as changes in surface area or volume are not required this allows them to pass through small pore with diameters much less than 8 μm. The normal shape of human red cell is a biconcave disk at rest (in unstressed situation), is approximately 8μm in diameter and varies in thickness from ~ 2.8 μm at the rim to ~ 1.4 μm at the center [24].
Figure 4 illustrated the shape of the red cell and Table 1summarizes typical dimensions. The Erythrocyte deformability is an important index of the blood flow in microcirculation.

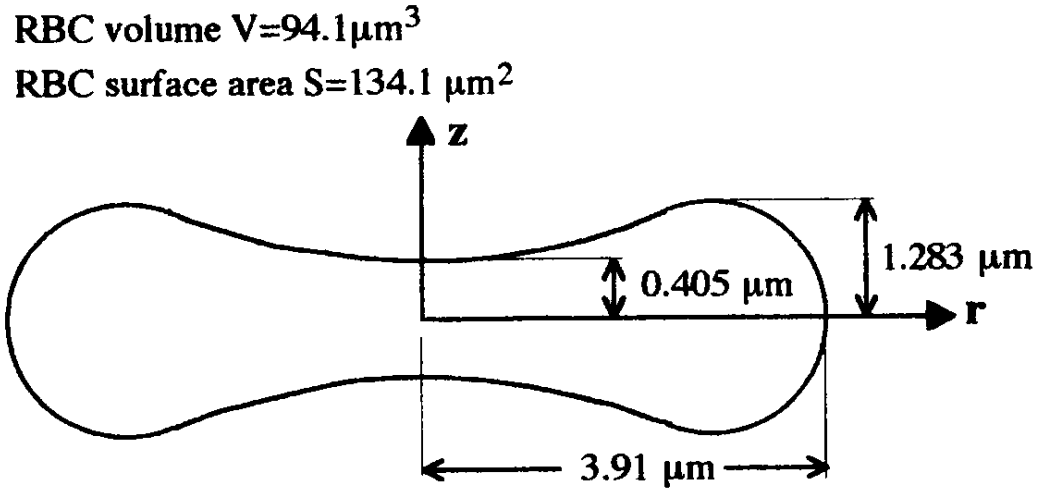

Figure 9.3
Shape and typical dimensions of a human erythrocyte.
Based on Evans and Fung [1972].

Figure 4: The shape and dimensions of the red blood cell [26]

Property	Value
Diameter	7.82±0.43 microns
Greatest thickness	2.56±0.15 microns
Least thickness	0.81±0.3 microns
Surface area	134.1±17 microns^2
Volume	94.1±17 microns^3

Table 1: Dimensions of the nominal red blood cell

- Leukocytes (WBCs)

The white blood cells (WBCs) are present in very low concentration, constituting about 1% of blood volume. The chief function of the WBCs is protection of the body against microorganisms causing disease. There are three varieties of white blood cells (WBCs) present in the circulation blood: granulocytes, monocytes, and lymphocytes, White cells are normally roughly spherical in shape, with the diameters of the different varieties of cell ranging from about 7 to 22 μm.

It has been founded that they are much stiffer than the RBCs, because in a collision between a red and white cell in flowing, it is the former that mainly deforms. The Leukocytes play an important mechanical role in capillaries and small vessels.

- Platelets

Platelets comprise about 4.9% of the cellular component of the blood; they are small round or oval bodies, ~2 to 4 μm in diameter and with volume of 5-10 μm^3. They play a major role in thrombogenic processes and blood coagulation, and do not contribute significantly to flow resistance.

- Plasma

Plasma is an aqueous solution of mostly proteins, is a pale yellow transparent fluid, which is obtained by removing the cells from the blood that has been prevented from coagulating. Normal human plasma is 92% water and 8% proteins and other inorganic substances.
Normal plasma behaves like a Newtonian fluid. Typical values for the viscosity of normal human plasma at 37° C is1.2 cP.

- Capillary

The capillaries are the smallest elements of the cardiovascular system and represent the site where the exchange of vital substances occurs between the blood and the tissues surrounding the capillary, the physical properties of typical capillary are summarized in Table 2 and the capillary wall, illustrated in
Figure 5, The capillary wall consists simply of a single layer of endothelial cells that surrounded by its basement membrane .the basement membrane is mat-like cellular support structure and has thick about 50-100 nm. The total thickness of the capillary wall is about 0.5 microns.

Property	Value
Inside diameter	10 microns
Length	0.1 cm
Wall thickness	0.5 microns
Average blood velocity	0.05 cm/sec
Mean pressure	17.3 mmHg (2.3 Kpa)

Table 2: Capillary properties

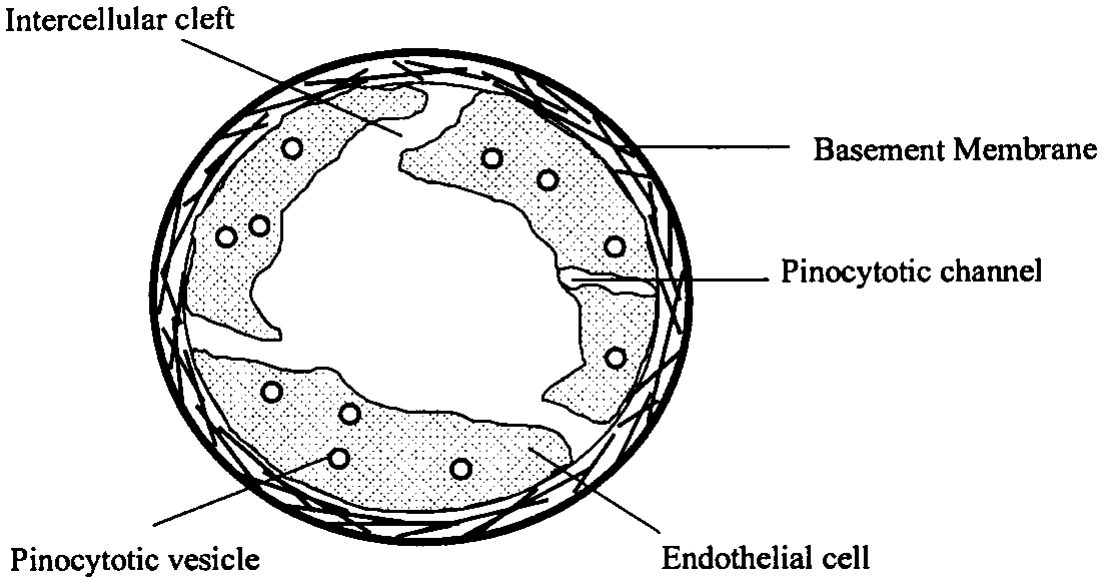

Figure 5: Cross-section of a capillary [25]

2.4.3 Blood Flow in Narrow Tubes

From a homodynamic point of view, critical property of microvessel is the resistant it presents to blood flow, defined as the ratio of the driving pressure ΔP to the volume flow rate Q [31].
For steady laminar flow of a Newtonian fluid in a cylindrical tube, Poiseuille's Law gives:

$$Q = \frac{\pi}{128}\frac{\Delta p D^2}{\mu L} \qquad [2\text{-}1]$$

Where L is the tube length, D is the diameter and μ is the fluid viscosity. In microvessels, however, μ is not a know constant, because blood does not behave as a continuum.
Resistance to the blood flow in microvessels is conveniently described in terms of the apparent viscosity, obtained by rearranging (equation [2-1]):

$$\mu_{app} = \frac{\pi}{128}\frac{\Delta p D^2}{QL} \qquad [2\text{-}2]$$

The relative e apparent viscosity is $\mu_{rel} = \mu_{app} / \mu_p$, where μp is the viscosity of the suspending fluid (plasma).

For glass tubes with diameters below about 500 μm, apparent viscosity is found to decline to levels substantially lower than the bulk viscosity, this known as the Fahraeus-Linndivist effect (Fahraeus-Linndivist, 1931). In the diameter 5 μm to 10 μm, μrel of human blood is below 1.3 cP.

2.4.4 Models for Blood Flow

The small size of microvessels implies that the Reynolds number is small, and the inertial effects can generally neglected. However, the particulate nature of blood has to be taken into account, the known mechanical properties of the individual red blood cells provide a basis for quantitative models.

3 Analytical Solution to Microchannel Flow

3.1 Basic Assumptions

After the following basic assumptions underlying the simple equation for flow in the channels: Consider first a steady flow of an incompressible (ρ= constant) Newtonian fluid in a rigid (It mean that the geometry is uninfluenced by the flow).

Flow within low Reynolds numbers, which are typical for the microcirculation makes it possible to neglect the inlet, outlet effects and consequently, justify the assumption of fully developed laminar flow.

3.2 Flow modeling

In this part the fundamental laws of fluidic element (Bernoulli and Navier –Stokes) are applied to micro-component in order to develop an analytical model (such as micro-channel "Trapezoid channel, Triangular channel and circular channel").

According to the theoretical models based on the Bernoulli equation, the total pressure drop ΔP across the channel is the sum of:

- The pressure drop due to laminar friction.

$$\left(\frac{1}{2}\rho U^2\left(\frac{L}{D_h}\right)f\right) \qquad [3\text{-}1]$$

- The pressure drop required for the acceleration or deceleration of the liquid.

$$\left(\frac{1}{2}\rho U^2 K\right) \qquad [3\text{-}2]$$

In our situation the pressure drop caused by acceleration or deceleration of the liquid is neglected because we working in low Reynolds numbers range and the ratio of the channel length to hydraulic diameter (L/ D_h) is bigger than the loss coefficient (k).

The pressure drop, ΔP, calculated using the law of friction for laminar flow and by rearranging (equation [3-1]) we obtained:

$$\Delta P = f\left(\frac{L}{D_h}\right)\frac{\rho U^2}{2} \qquad [3\text{-}3]$$

By definition

$$U = \frac{Q}{A} \qquad [3\text{-}4]$$

Reynolds number, $R_{e,}$ based on hydraulic diameter, $D_{h,}$ of the microchannel. Re_{Dh} is the ratio between the inertial and the viscous forces affecting the fluid flow.

$D_{h,}$ is a factor used to approximate a non –circular microchannel to a circular microchannel.

$$D_h = \frac{4A}{P} = \frac{cross-\text{sec}tional\ \text{area}}{\text{wetted perimeter}} \qquad [3\text{-}5]$$

$$\text{Re}_{D_h} = \frac{\rho Q D_h}{A\mu} \qquad [3\text{-}6]$$

In equation [3-6] ρ is the fluid density and μ is the fluid dynamic viscosity. Where, C friction factor constant

$$C=f.\ Re \qquad [3\text{-}7]$$

is parameter depending on the geometric shape and L is the channel length.

By plugging [3-4], [3-5], [3-6], [3-7] into the expression for ΔP is obtained.

$$\Delta P = \frac{C}{2}\frac{L\mu}{D_h^{\,2}}\frac{1}{A}Q \qquad [3\text{-}8]$$

The equation for flow rate, Q, through microchannels is:

$$Q = A\frac{2}{C}\frac{D_h^{\,2}}{L\mu}\Delta P \qquad [3\text{-}9]$$

For different and noncircular cross-section the friction factor constant *C*, data can be found in the literature [7] and [30]. A resistance to flow in fully developed flow through straight microchannels of various cross-sectional geometries is shown in appendix A. The Pressure gradient is assumed to be constant across the microchannel length can be calculated. As shown in equation [3-10], $\frac{dp}{dx}$ is the product of pressure drop and total microchannel length, *L*.

$$\frac{dp}{dx} = \frac{\Delta P}{L} \qquad [3\text{-}10]$$

Furthermore, microchannel resistance, R, is the driving force divided by the flow rate as shown in equation [3-11].

$$R = \frac{\Delta P}{Q} \qquad [3\text{-}11]$$

4 Research Objectives

The research aim is to investigate microcirculatory this through the investigation of the flow in microchannels for several cases.

The study will be conducted using the following steps:

- Develop and fabricate a Lap-Biochip including microchannels, which – accounts for the most essential microstructural and geometrical features of microcirculation.
- Using the Lap-Biochip to investigate the microcirculatory parameters.
- Develop and fabricate experimental methodology to investigate Microfluidics.
- Comparing various fluids.

5 Experimental Work

5.1 Test module fabrication process

5.1.1 Micromachining Technology

Mostly micromechanical devices have been fabricated using silicon micromachining. Historically silicon has been the most commonly used material in MEMS. The fabrication methods originate from IC manufacturing. Silicon micromachining is usually divided into bulk micromachining and surface micromachining .In bulk micromachining the whole thickness of the silicon wafer is structured while in surface micromachining all the fabrication is done on the surface.

The most important manufacturing process steps in micromachining and used during this work are summarized below:

Lithography

In the first step a mask is defined on the silicon using a photolithographic process. This mask defines the pattern that should be etched. Different materials can be used as mask materials depending on the following type of process. Silicon dioxide and silicon nitride are probably the most commonly used mask material, but for dry etching it is also common to use photoresist or a deposited metal, e.g., chromium.

Etching

In the next step the actual etching of the silicon is done. The etching can be done using wet or dry etching. Different etches give different etch profiles as shown in Figure 6.

Wet isotropic etching

Wet isotropic etching ideally is direction independent. How ideal the isotropy is depends on how the etching solution is composed and how the reactants are transport to and from the etching front. A less agitated etching gives flatter bottom. The etching solution is normally based on fluoric (HF), nitric (HNO3) and acetic acid (CH3COOH). A typical etch profile is shown in Figure 6-a. Silicon dioxide is not useful as mask material since the HF etches it. Instead silicon nitride, Si3N4, is normally used as the mask material. Isotropic etching is commonly used for chemical polishing of wafers.

Wet anisotropic etching

Wet anisotropic etching is based on the fact that the etch speed in single crystalline silicon is direction dependent. Examples of anisotropic wet etches on silicon are EDP (ethylene diamine, pyrocatechol and water), KOH (potassium hydroxide and water) and TMAH (tetramethyl ammonium hydroxide and water). Typical etching results for KOH are shown in Figure 6-b.

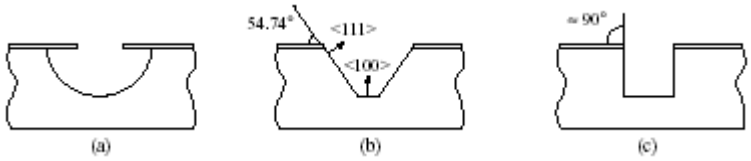

Figure 6: Cross-sectional views of (a) isotropic etch, (b) and (c) anisotropic etch with profiles dependent on the crystal planes and etch method.

Where the etching has stopped at the (111) plane. This result is obtained when the mask is oriented parallel to the <110> directions for (100) surface oriented silicon wafers. A result similar to that shown in Figure 6-c is obtained if the mask is oriented ± 45° to these directions, i.e. oriented parallel to the <100> direction.

Deep reactive ion etching (DRIE)

Dry etching or reactive plasma etching of silicon is common in micromachining technology. The etching is performed in a chamber at a pressure of 0.5 to 25 Pa. The term reactive plasma describes a discharge in which ionization and fragmentation of gases take place and produce chemically active species. Such plasmas are reactive both in the gas phase and with solid surface exposed to them. These interactions are used to form volatile products so that material is removed or etched from surfaces that are not masked by lithographic patterns. The interactions can be divided into two types: physical and chemical. The physical interaction refers to the surface bombardment by energetic ions accelerated across the sheath. Chemical interactions are standard electronic bonding process that result in formation or dissociation of chemical species on the surface. Generally the chemical etching is isotropic and the mechanical sputtering is anisotropic. Most reactive ion etches are based on chlorine or fluorine processes and common gases are SF6 and Cl2.

A cross-section of an etching profile is shown in Figure 6-c.

Deposition

A microsystem typically consists of various materials integrated to perform different functions. The conventional methods for depositing materials on the surface include sputtering, evaporation and chemical vapor deposition. These methods are carried out in a low pressure (~10-8 Torr) environment. The choice of the method depends on the material deposited, the type of the film required (e.g. uniform, thick) and conditions the substrate can withstand (temperature, pressure).

Anodic bonding

Anodic bonding can be used to bond a silicon wafer and a glass wafer together [2]. The glass is normally a sodium glass like corning 7740. The bonding is carried out at a temperature between 180°C and 500°C when an external voltage in the range 200-1000V is applied. Observing the current can monitor the bonding process. When the voltage is applied the current starts with a peak and then decreases. The bond will normally be good when the current has reached about 10-30% of the initial value. Normal bonding time is about 5-10 minutes, but up to half an hour can be necessary. The principle is shown in Figure 7.

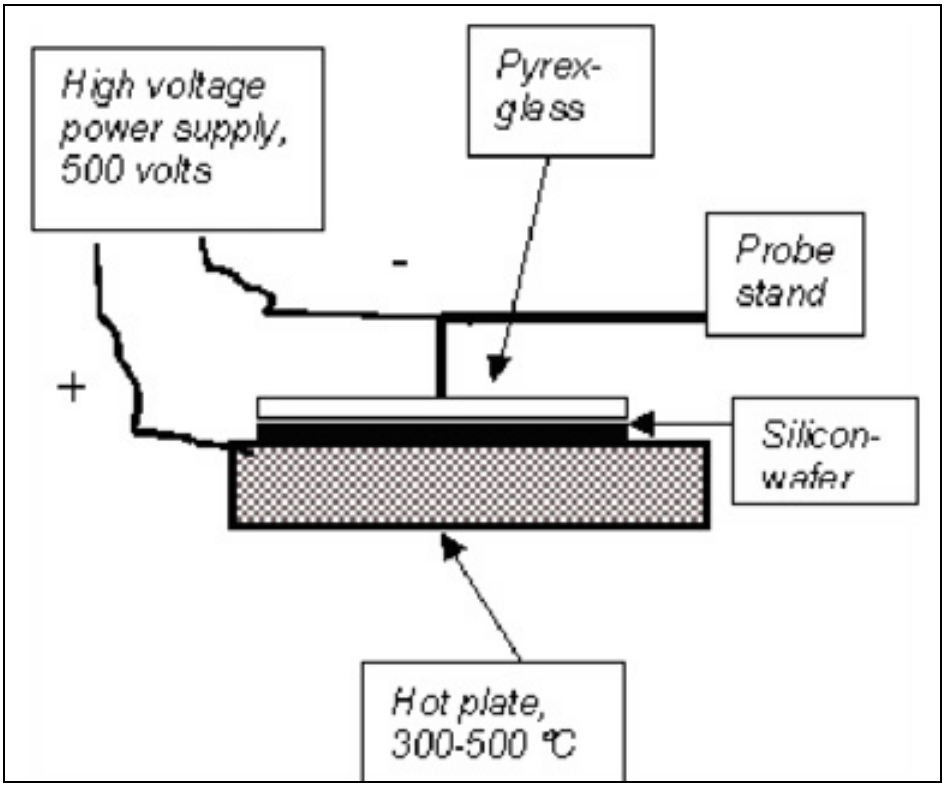

Figure 7: Anodic bonding principles

Materials

Inorganic, organic and biological materials are used to construct the microsystem and give functional features (for e.g. sensors, valves). The choice of the material depends on its bulk and surface properties and compatibility with other materials. The main requirement of the substrate is that must be easy to fabricate. The materials that are commonly used for fabricating the microsystem are listed in Table 3.

The main bulk properties are transparency, strength and hardness of the material. Transparency is required to allow detection like fluorescence spectroscopy. Strength and hardness of the material will characterize the capability and limitations of the materials. For example; high pressures cannot be used with microsystems made with PDMS. The main surface properties are the surface energy, charge and reactivity. These properties will dictate the compatibility between the materials. Compatibility issues arise due to lack of adhesion between materials, difference in thermal conductivities creating bends and cracks, and their reactivates. PDMS is a commonly used material for making a microsystem and many fabrication methods.

Material	Property	Fabrication Method
Silicon	Hydrophobic (SiO_2 layer on surface makes it hydrophilic), semiconductor, transparent in infrared region	Photo-patterning PR and etch
Glass (types – Pyrex, fused, quartz)	Hydrophilic, insulator, transparent in UV-visible region	Photo-patterning PR and etch
PDMS	Hydrophobic (made hydrophilic by treatment with oxygen plasma), transparent in UV-visible region	Mold from master
EPON (epoxy resin)	Hydrophobic, positive PR, allows high aspect ratio, yellowish color, less transparent, hard	Photo-patterning and develop

Table 3: Materials properties and fabrication methods

5.1.2 Microchannels Fabrication Process

The Microchannels used in experiments with circular cross section but different diameter. The microchannels are micro machined and etched in silicon using the DRIE (Deep Reactive Ion Etching). All the microchannels were covered with Pyrex glass using gluing techniques.

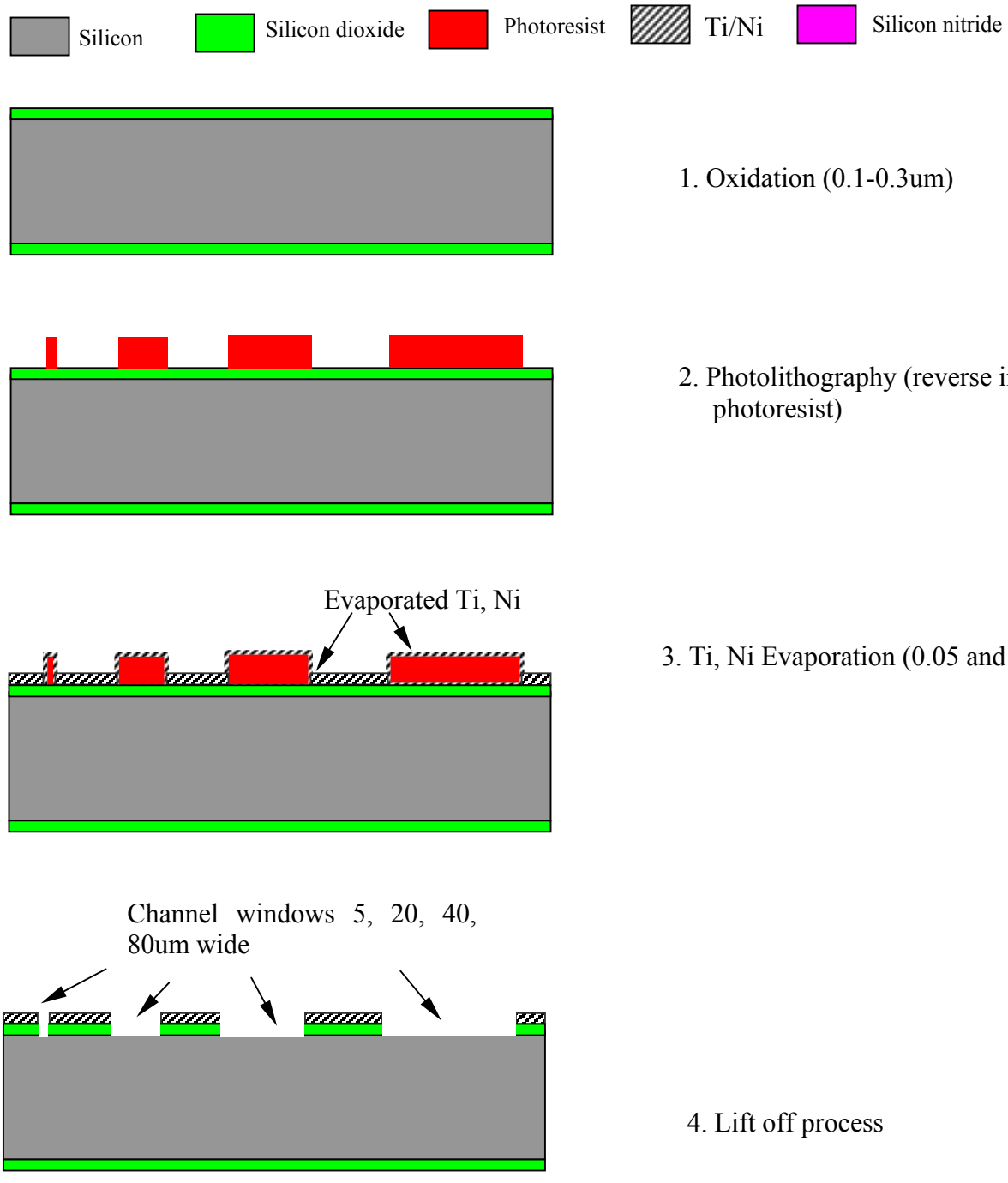

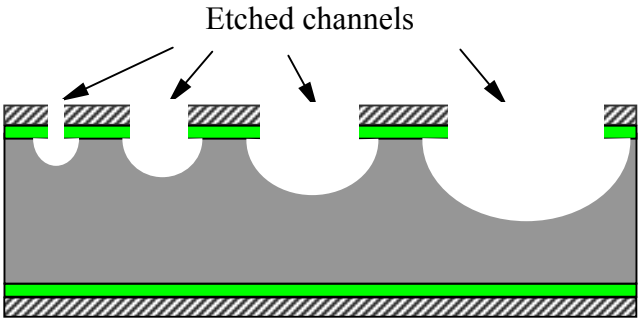

5. Isotropic silicon plasma etching

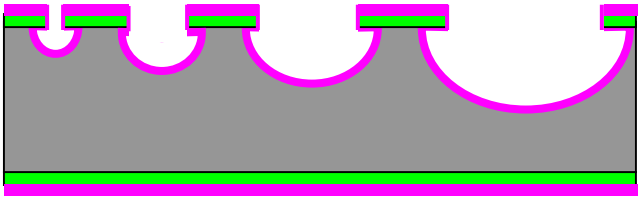

6. Nitride deposition

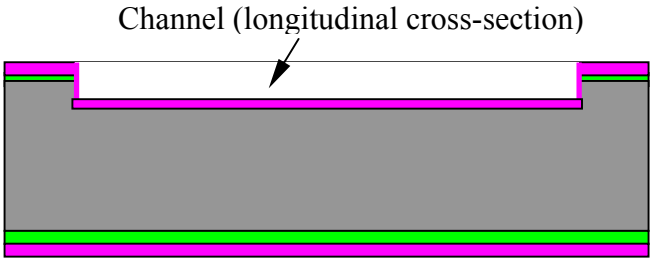

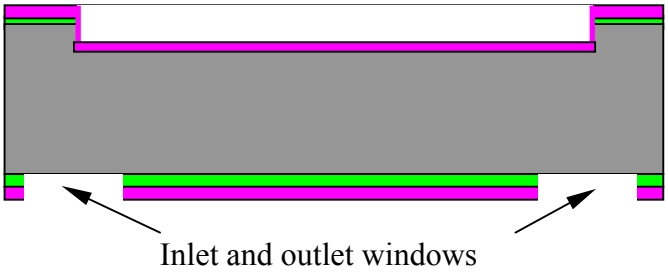

7. Inlet-outlet patterning at the back of the wafer

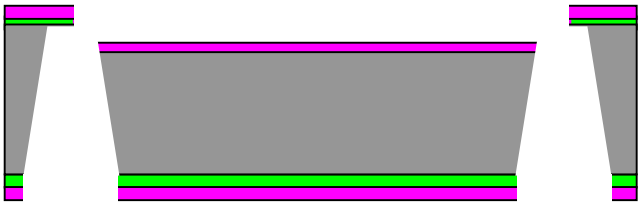

8. Anisotropic etching of the inlet and outlet

9. Stripping off the nitride and oxide

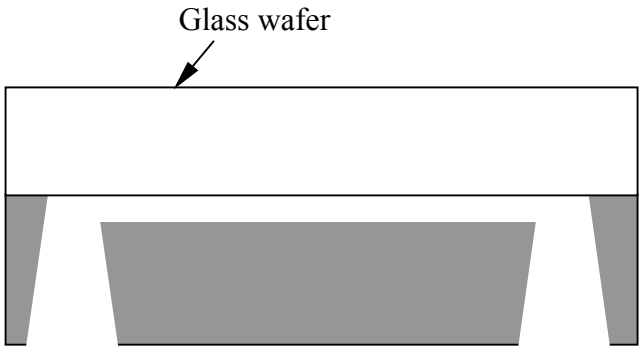

10. Gluing to a glass wafer

5.1.3 Gluing Technique of the Microchannels

1. Dispensing the UV-curable glue on the glass slip

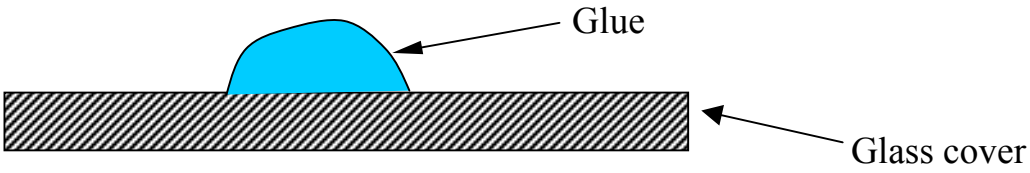

2. Spinning (8000-9000rpm) for 1min. measured glue thickness was 2-3um.

3. Placing upon the silicon chip with channels, applying the force of (5 kg) and exposing to UV light for 10min.

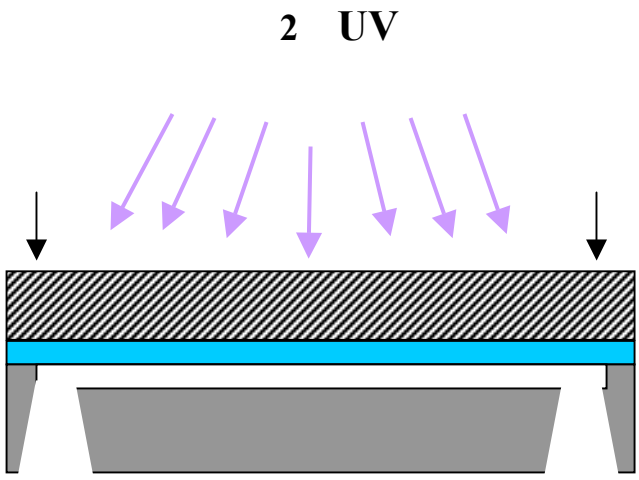

5.1.4 CAD Tools for microchannels and system design

CAD (**Computer Assisted Design)**

The 3D design and the 2- dimensional layouts, or the masks, of the microchannels were generated using software called SolidWorks (SolidWorks Corporation, USA).

The software converts the layout of the microchannels into format, which is a commonly accepted format for mask making. The SolidWorks drawings for mask and microchannels are shown in Figure 8.

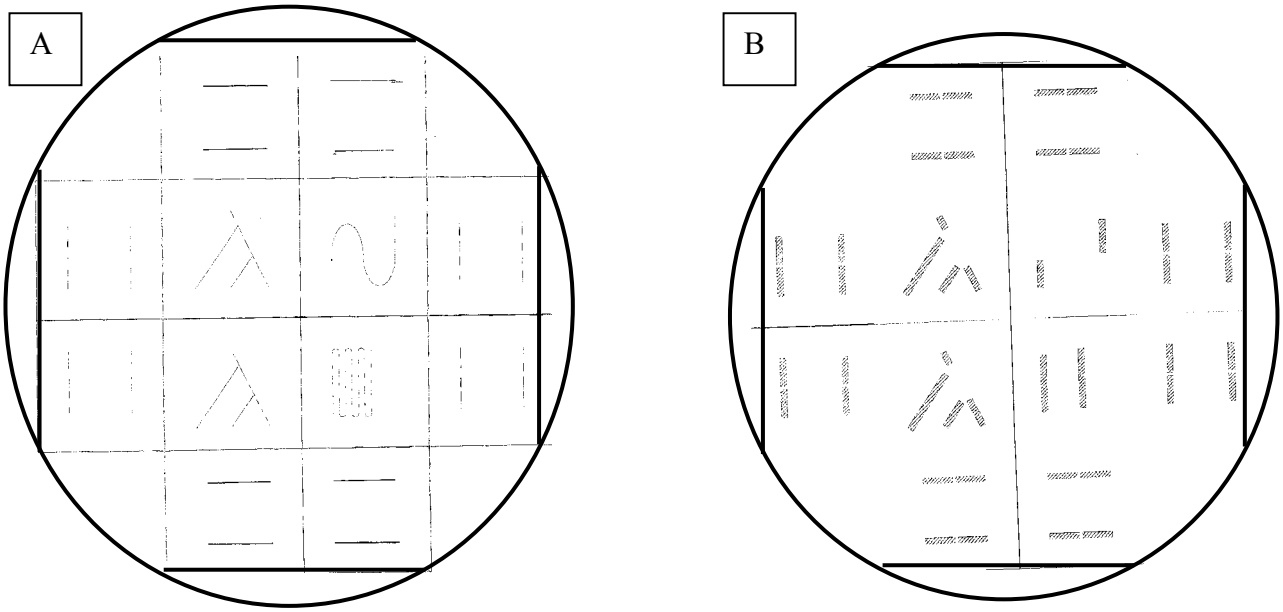

Figure 8: A) SolidWorks drawing of microchannel on 4 inch in diameter silicon wafer, The drawing shows the three types of the test module per wafer, eight modules of straight microchannel with different sizes, two modules of looped microchannel, two modules of bifurcated microchannel with different sizes, twelve modules in total. B) SolidWorks drawing of the mask of microchannel used during photolithography, the circle around the mask indicates the silicon wafer.

5.1.5 Packing and Interfacing to the Macro-World

A rigid assembly shown in Figure 9 below was fabricated in order to packing and interfacing the module to the macro-world and be ready for fluid study. The assembly not only stabilized the silicon chip, but also provided the fluid access to the microchannels. The parts of this package were the aluminum base adapter, the module itself, and two in /out adapters.

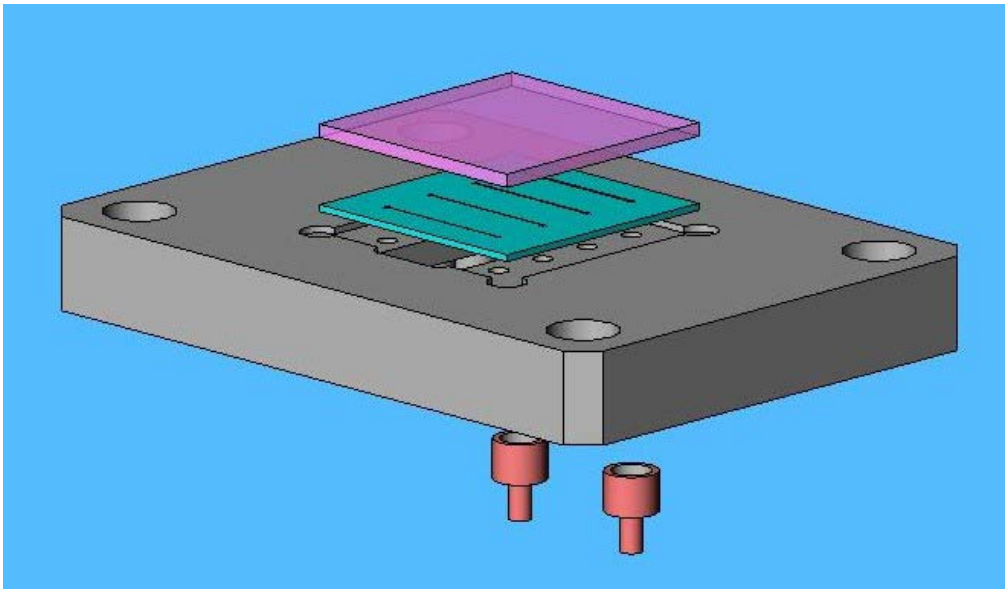

Figure 9: Packaging and fluid access of module showing the aluminum base adapter, module test, and in /out adapters.

The base adapter is an aluminum rectangle that is 55 mm x 40 mm x 7 mm thick with a 19 mm x 19.5 mm x 0.5 mm square hole, called the pocket, milled into its center. This pocket is where the module sits by gluing technique. To create the input and output ports in the base adapter, 1.5 mm diameter holes were drilled into opposite sides of the base adapter. These holes stop directly under the location where the fluid ports of the module will lie. A dimensional drawing of the base adapter is shown in Appendix B.

After the gluing of the module on the pocket and create a sealed fluid circuit. After the seal is created, silicon tubing connected to the fluid ports in the aluminum base adapter. The assembly is then ready to be placed on the experimental setup.

5.2 Experimental Apparatus and Procedure

5.2.1 Microchannel Test Module

The liquid is led to the inlet of Microchannel Test module, which consists of a Silicon wafer, Pyrex glass and metallic adapters for inlet and outlet of the liquid.

The microchannels etching basically done by two ways, it depends on the cross-section of the microchannel. Microchannel was etched with Anisotropic etching in a KOH solution, resulting in a triangle and trapezoidal cross-section in which the <111> planes intersect the wafer surface at angle of 54.7`. Microchannel was etched with isotropic silicon plasma etching, resulting in a Semi-circular cross-section. The inlet and the outlet of the microchannel were etched with anisotropic etching. The etched silicon wafer is covered with Pyrex glass using Gluing Techniques and Anodic bonding Techniques.

The test module assembly is shown in Figure 10.

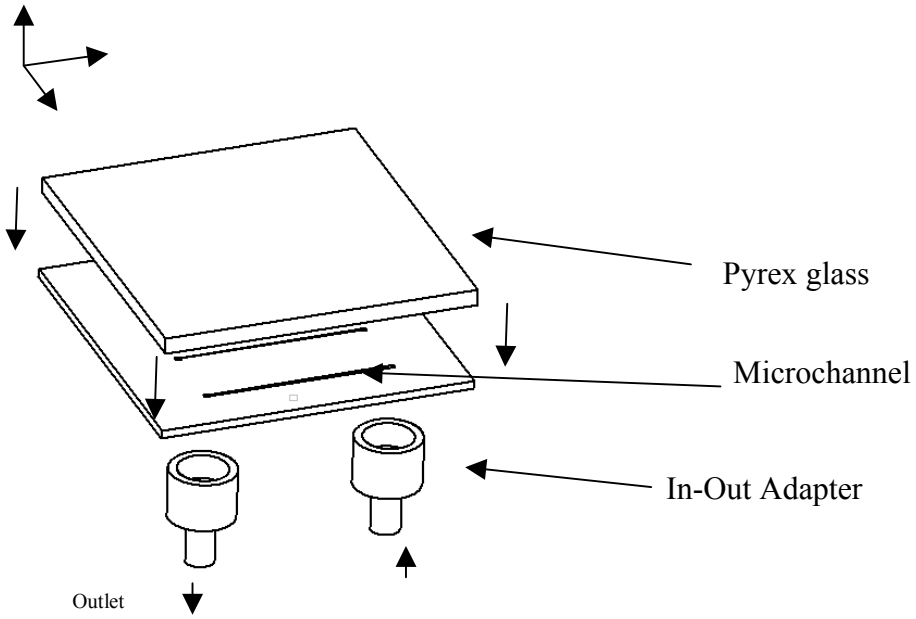

Figure 10: Close view of Microchannel Test module

5.2.2 Microchannel Cross-Section

In this study checked three difference Microchannel Test Module cross-sections:

- Triangular cross-section:

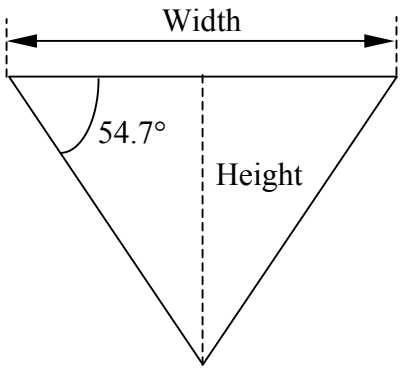

Figure 11: Test module Triangular cross-section

The parameters of Triangular cross-section used in equation [3-5] are:

$$A = \frac{(a+b)h}{2} \qquad [5\text{-}1]$$

$$P = a + b + 2\sqrt{h^2 + \frac{(a-b)^2}{4}} \qquad [5\text{-}2]$$

Where ***a*** is the width and ***h*** is the height of the Triangular.

b=0 in this situation , it is the base of trapezoid cross section.

Channel	*Channel Width [μm]*	*Channel Height [μm]*	*Hydraulic diameter Dh [μm]*
A	95	67.09	49.14
B	66.6	47.03	34.45
C	45.5	32.13	23.53
D	32	22.60	16.55

Table 4: Test module channels Triangular cross-section dimensions and parameters

- Trapezoid cross-section:

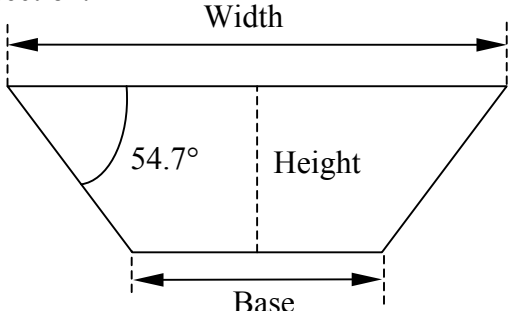

Figure 12: Test module Trapezoid cross-section

The parameters of Trapezoid cross-section used in equation [3-5] can calculate by using equations [5-1] and [5-2].

Where ***a*** is the width and ***h*** is the height of the trapezoid.

b is the base of trapezoid .

Channel	*Channel width top [μm]*	*Channel Height [μm]*	*Hydraulic diameter Dh [μm]*
E1	150	40	57
E2	80	20	29

Table 5: Test module channels Trapezoid cross-section dimensions

- Semi-circular cross-section:

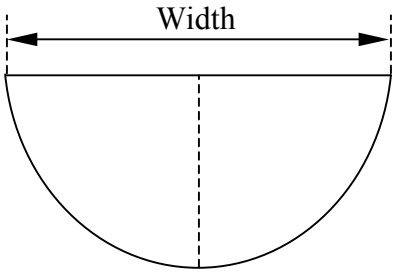

Figure 13: Test module Semi-circular cross-section

The parameters of Triangular cross-section used in equation [3-5] are:

$$A = \frac{\pi a^2}{8} \qquad [5\text{-}3]$$

$$P = \frac{\pi a}{2} + a \qquad [5\text{-}4]$$

Where ***a*** is the width of the Semi-circular.

Channel	***Channel width top [μm]***	***Channel length [μm]***	***Hydraulic diameter Dh [μm]***
R1	80	21500	48.8

Table 6: Test module channels Semi-circular cross-section dimensions

5.2.3 Test module concepts:

In this study checked three difference Microchannel Test Module concepts:

1. Branching Channels

$$Q_{in} = Q_{out-1} + Q_{out-2} + Q_{out-3} \quad [5\text{-}5]$$

2. Straight Channels

$$Q_{in} = Q_{out} \quad [5\text{-}6]$$

3. Loops Channels

$$Q_{in} = Q_{out} \quad [5\text{-}7]$$

1. *Test module Branching Channels*

Channel	*Channel Width [μm] Sample 1*	*Channel Width [μm] Sample 2*
A	15	30
B	7	10
C	3	5

Table 7: Test module Branching Channels samples 1 and 2 dimensions

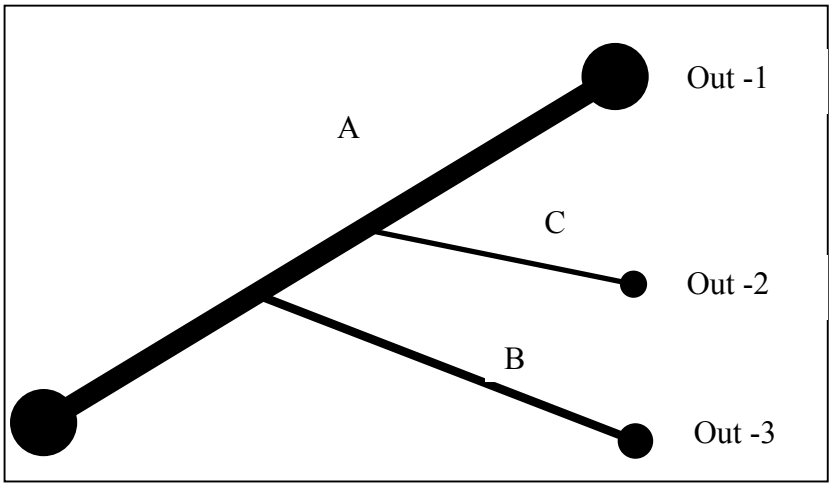

Figure 14: Test module Branching Channels

2. *Test module Straight Channels*

Channel	*Channel Width [μm]*
A	80
B	40
C	10
D	5

Table 8: Test module Straight Channels dimensions

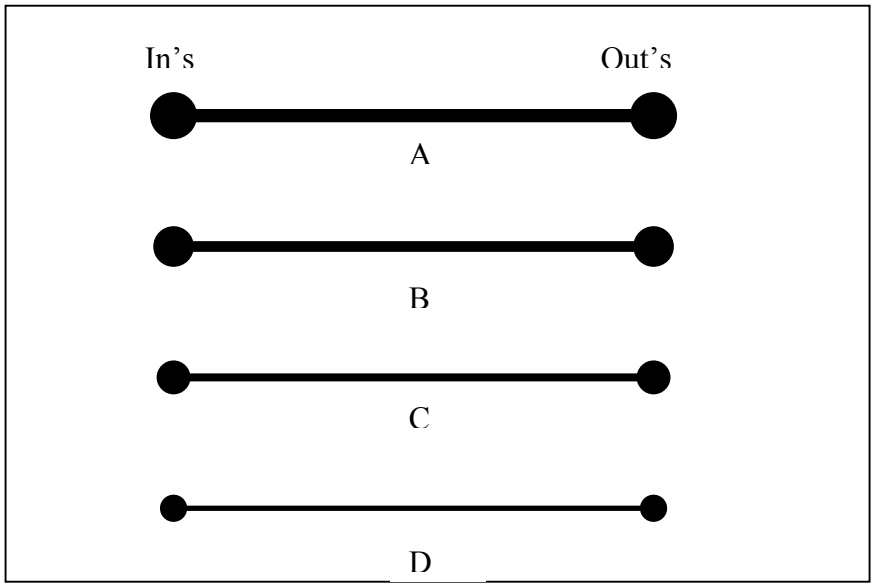

Figure 15: Test module Straight Channels

3. *Test module loops Channels*

Sample	*Channel Width [μm]*	*Loops numbers*
1	7.5	2
2	7.5	3

Table 9: Test module Loops Channels samples 1 and 2 dimensions

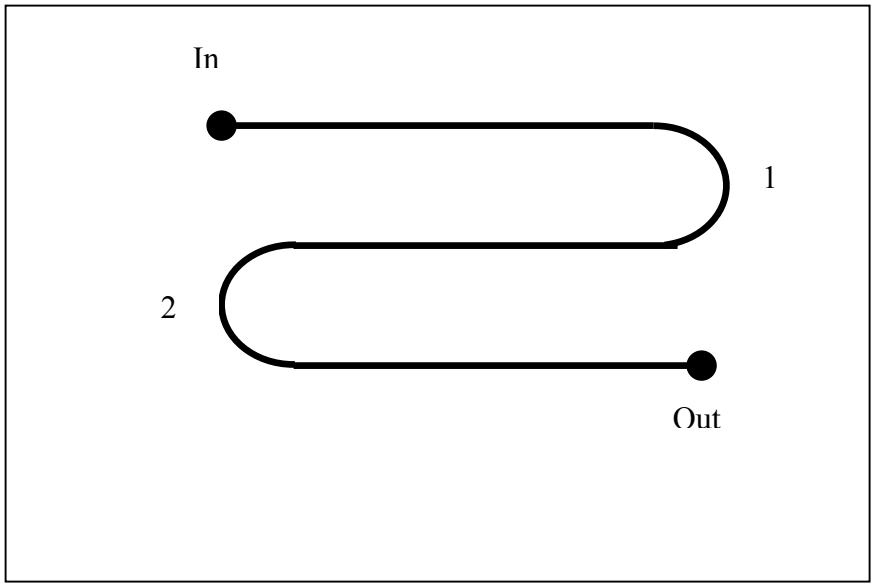

Figure 16: Test module Loop Channel sample 1

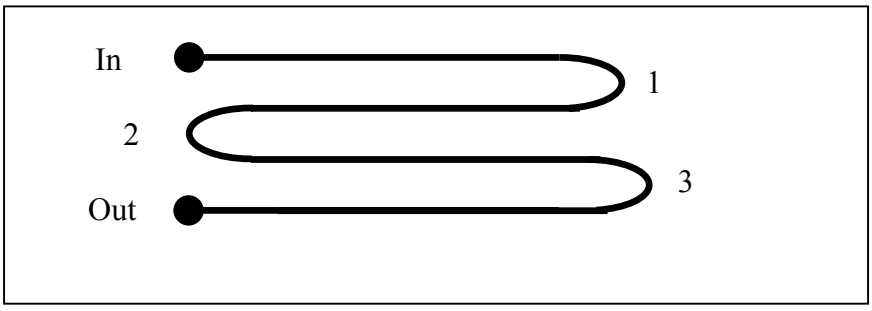

Figure 17:Test module Loops Channel sample 2

5.2.4 Experimental Procedure

The experimental apparatus used in the study is shown in Figure 18.all the experiments were carried out in clean room, where the ambient temperature is under careful control. The experimental apparatus consists of a pressurized air (compressor), two (coarse and fine) pressure regulators, two (oil and water) filters, a digital pressure transducer, a liquid reservoir and Microchannel Test Module.

The experiments designed in this communication mainly focus on investigating the relation between Q and ΔP under relatively lower pressure when characteristic size of the channel scaled down and the cross section changed.

To fulfill the measurement, a micro-fluid measurement system has been developed, Inlet pressure controlled by two pressure regulators (SMC Co. Japan, EAW3000-F02, EARP3000-F02) upstream to the Microchannel Test Module. The air is supplied from the compressor and flows through the coarse pressure regulator. The pressure of the air is reduced down to a proper pressure level before entering to the precision pressure regulator, were the inlet pressure controlled precisely. To avoid clogging, liquid need to pass through two filters (oil and water) regarding to whole air path lines (SMC Co. Japan, EAW3000-F02, EAFD3000-F02), following the air enter to the liquid reservoir made from Perspex plate cleaned and pressurized, on the liquid reservoir installed a digital pressure transducer (AMR Co. Germany, FD 8214 M and 2190-2), so the liquid led to the inlet of the Microchannel Test Module, after leaving the Microchannel Test Module the liquid pass to small container.

After confirming that the flow on steady state, the time was measured using a stopwatch and the container was balanced by analytical balance (METTLER TOLEDO Co. Switzerland, AB204-S).

The volumetric flow rate was obtained by averaging the readings of the container weight on a constant time.

Any other way to measure the volumetric flow rate, the fluid pass through a scaled pipe all the way to the container, on a constant time the volumetric flow was taken and calculates the flow rate.

The pressure difference between the inlet and outlet of the Microchannel Test Module was measured using a digital pressure transducer (AMR Co. Germany, FD 8214 M and 2190-2). Pressure loss in the supplying line other than in the microchannel can be neglected due to much larger cross-section of the line and thus due to the negligibly small flow velocity there, compared to those in the microchannel. The measure value from the digital pressure transducer was taken as the pressure difference along the microchannel.

The accuracy of the pressure transducer, given by the supplier, is 0.5% of a full scale.

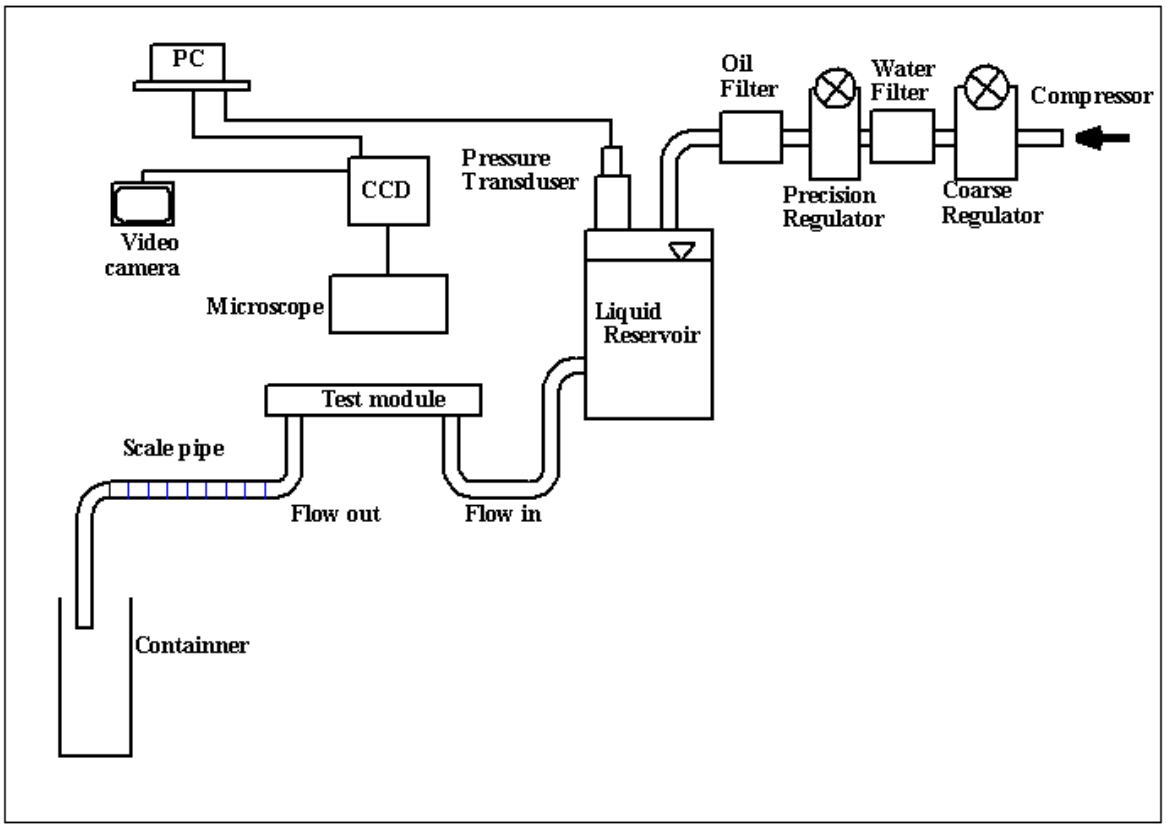

Figure 18: Schematic Descriptions of the Experimental Apparatus

Fluids

We used different fluids in our experiments. To verify that the microchannels were fabricated fine and can used for the experiment, we perform verification test with first fluid Distilled Water.

The results used to approved the microchannels and for comparison purposes. The second fluid was Ethanol which his viscosity similar to the plasma. The third was Isopropanol and the last is Glycerin.

Fluid name	Density, ρ[kg/m^3]	Viscosity, μ [kg/(m.s)]
Distilled Water	998@ 20°C	1.00E-3 @ 20°C
Ethanol (Absolute)	789@ 20°C	1.20E-3@ 20°C
		1.26E-3@ 25°C
Isopropanol	785.05@ 20°C	2.04E-3@ 25°C
Glycerin	1261@ 20°C	1.49@ 20°C

Table 10: Fluid properties at 20°C and 1 atm. of the fluids used in flow experiments.

Flow measurements

The experimental data were obtained for water flows at room temperature with Reynolds numbers *Re* in the 10 to 60 ranges.

During the experiments, the measured parameters were the flow rate *Q* and pressure drop across the microchannel *ΔP*.

Others parameter used to describe the flow characteristics, such as pressure gradient $\frac{dp}{dx}$, Reynolds number *Re,* friction factor *f* and friction factor constant *C,* can be easily related to these two measured parameters as follows.

6 Results and Discussion

The results will include the following sections:

1. Microchannels and Fabrication of microchannels
    a. Microchannels
    b. Fabrication of microchannels
    c. Microchannels Manufactured and Tested
2. Flow measurements
    a. Flow Rate Vs. Pressure Drop
    b. Pressure Gradient Vs. Reynolds Number
3. Comparing various fluids
4. Improvements to Microchannel System

6.1 Microchannels and Fabrication of microchannels

6.1.1 Microchannels

The microchannels developed satisfy the objective to develop rigid microchannels for the study of microcirculation and the characterization of flow rheological properties. It has been shown that microfabrication techniques provide the geometric control and minimum dimensions required to create a microfluidic network. The microchannels isolated the extensive microcirculation into two parts; to study the effect of microvessel size, and the effect of microvessel geometry on flow. To isolate microvessel size, straight microchannels of various widths and cross sections were designed. To isolate microvessel geometry, bifurcated and looped microchannels were designed.

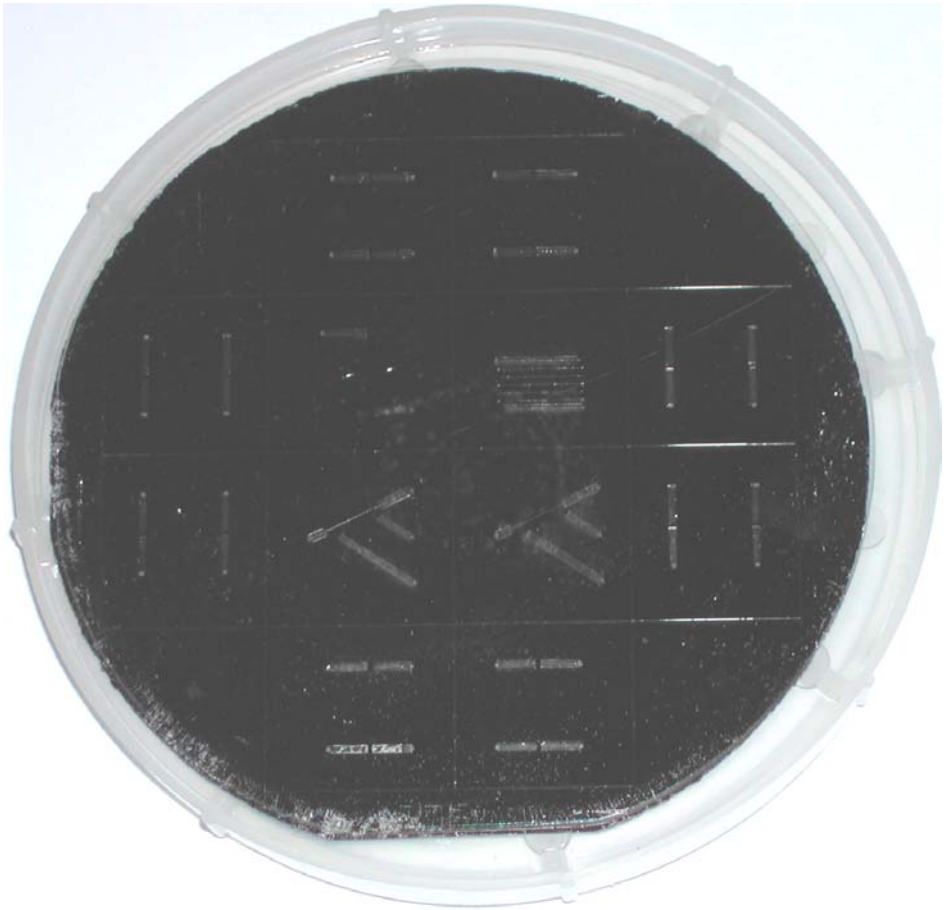

Figure 19: Picture of wafer include three types of the test module per wafer, eight modules of straight microchannel with different sizes, two modules of looped microchannel, two modules of bifurcated microchannel with different sizes, twelve modules in total.

6.1.2 Fabrication of microchannels

Fabrication of the microchannels was successfully performed at the Microelectronics Research Center at Technion-Israel Institute of Technology.

Pictures of the four types of microchannels are shown in Figure 20.

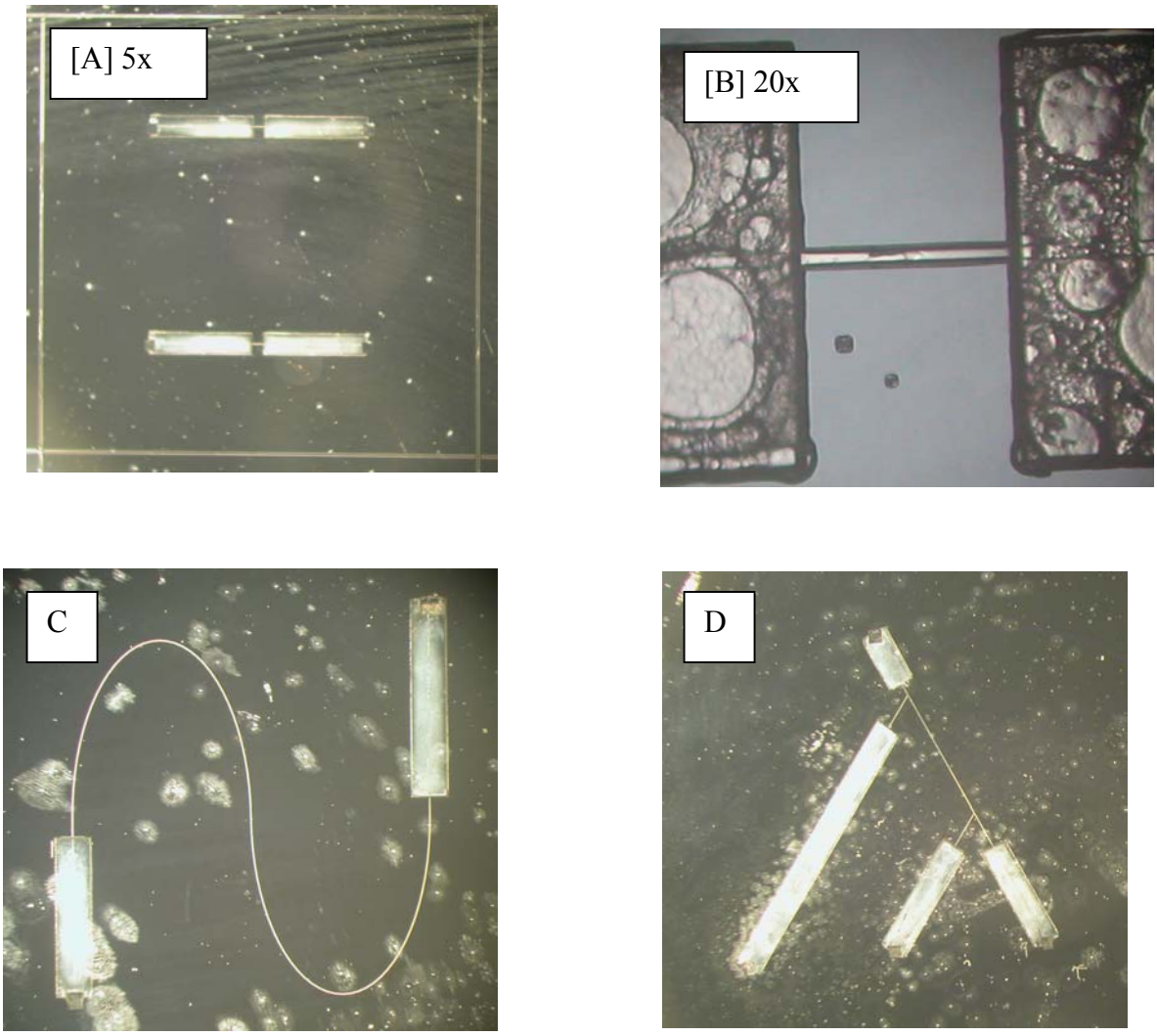

Figure 20 : Selected pictures of microchannels. A) 66 µm wide straight microchannel B) 20 x zoom of 66µm wide straight microchannel. C) 80 µm wide Looped microchannel. D) 55 µm wide bifurcated microchannel, 55 µm wide microchannel that bifurcated into a 32 µm wide microchannel and a 16 µm wide microchannel.

These 2- dimensional pictures show that the microchannel configurations were etched sharply. While 2- dimensional microchannels pictures were obtained with incident light microscopy.

6.1.3 Microchannels Manufactured and Tested

Channel	***Width [μm]***	***Height [μm]***	*Friction factor constant (C=f. Re)*	*length L [mm]*	***Hydraulic diameter Dh [μm]***
A	95	67.09	53.1	11.02	49.14
B	66.6	47.03	53.1	11.02	34.45
C	45.5	32.13	53.1	11.02	23.53
D	32	22.60	53.1	1.102	16.55

Table 11: Test module Straight microchannels with Triangular cross-section dimensions and parameters

Channel	***Width top [μm]***	***Height [μm]***	*Friction factor constant (C=f. Re)*	*length L [mm]*	***Hydraulic diameter Dh [μm]***
E1	150	40	65.5	11.02	57
E2	80	20	67	11.02	29

Table 12: Test module Straight microchannels with Trapezoid cross-section dimensions and parameters

Channel	***Width top [μm]***	***Length*** *L [mm]*	*Friction factor constant (C=f. Re)*	***Hydraulic diameter Dh [μm]***
R1	80	21.5	63	48.8

Table 13: Test module loped microchannels with Semi-circular cross-section dimensions and parameters

6.2 Flow measurements

6.2.1 Flow Rate Vs. Pressure Drop

We investigate the flow of Distilled water in straight microchannel, with different Triangular Cross-Section sizes, hydraulic diameters ranging from 16.55 to 49.13 μm, each graph includes the results obtained for the 11 mm length Microchannels.

The results of the measurements of the flow rate as a function of the pressure drop are present in Figure 21, for each measured flow rate; the theoretical pressure drop is calculated from the conventional theory. A comparison between the experimental data and the theoretical predicted curves is shown in Figure 21.

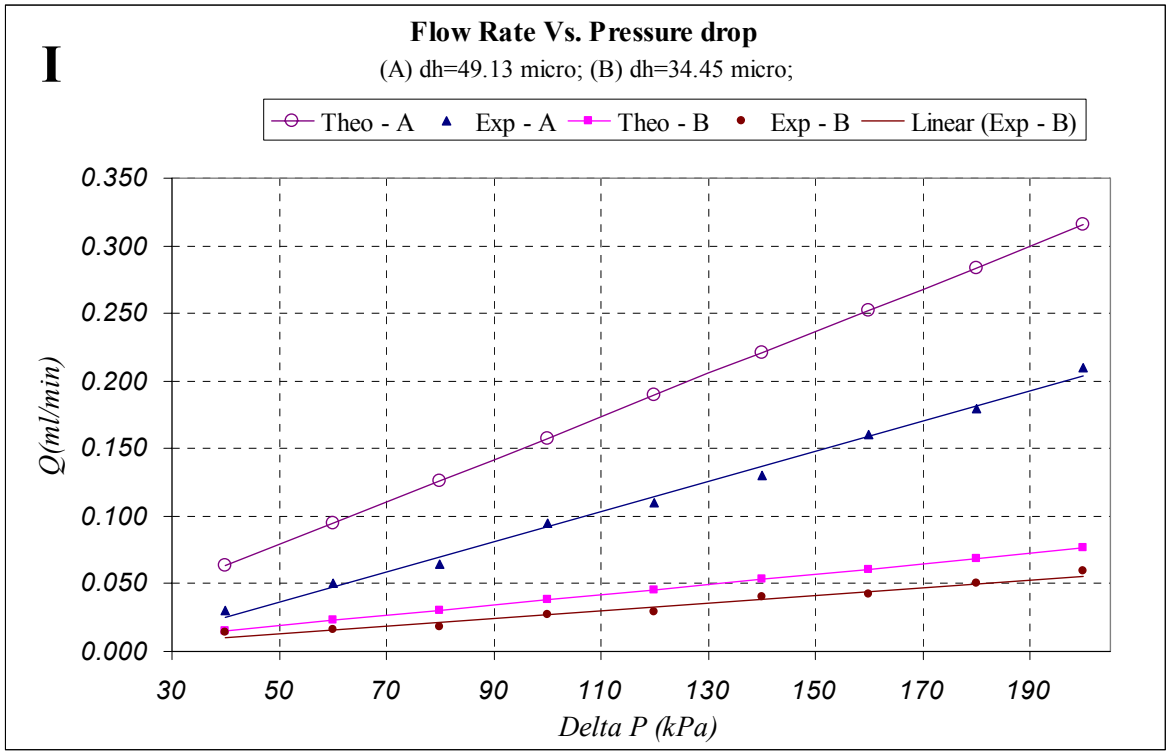

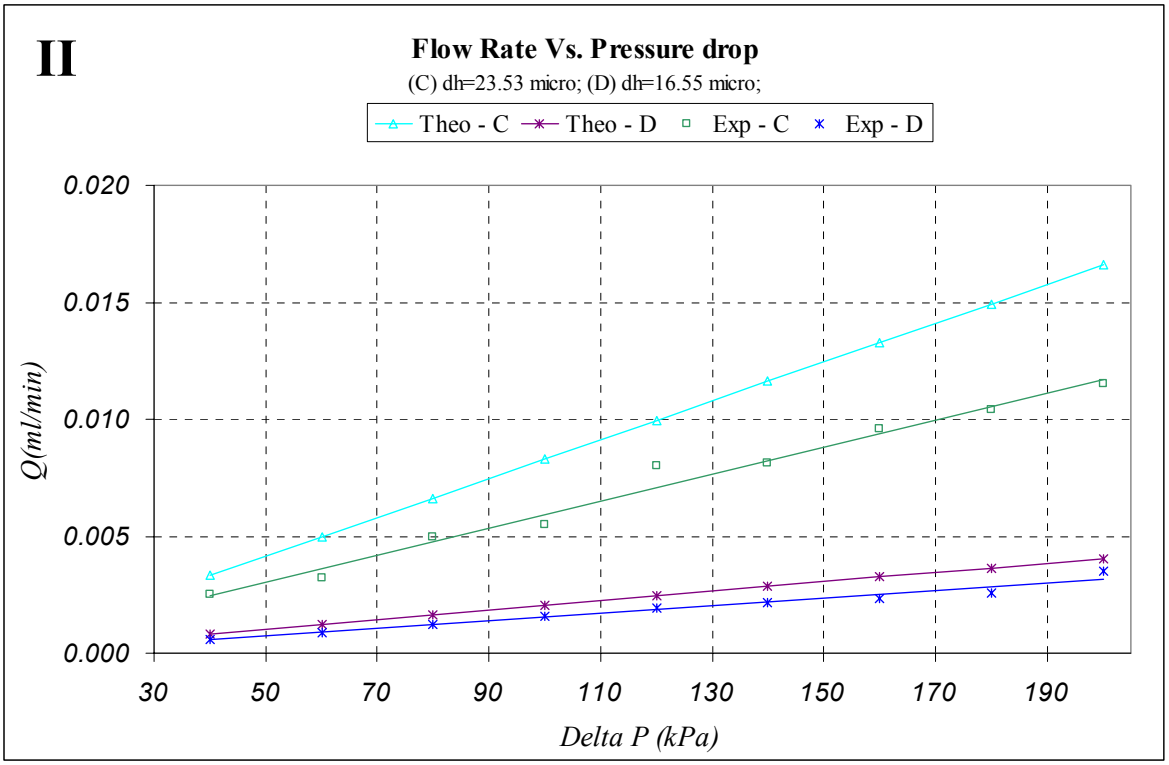

Figure 21: A Comparison of the measured data of flow rate vs. Pressure drop with the prediction of conventional laminar flow theory. Distilled water Flow in Triangular Cross-Section Microchannel with the Hydraulic diameters, I (A) dh=49.13 μm; (B) dh=34.45 μm; II (C) dh=23.53 μm; (D) dh=16.55 μm;

A comparison is made between the experimental data obtained for Microchannels of hydraulic diameters ranging from 16.55 to 49.13 μm, and the calculation flow based on conventional fluid mechanics.

The calculation essentially describes the relationship of flow rate to pressure.

Figures 21(I) - (II) indicate that, for Microchannels of dimensions considered, the calculation in this study based on the conventional fluid mechanics, can adequately predict the resulting flow chrematistics of the triangular Microchannels.

It should be noted that the experimental curves are all linear as required by conventional laminar flow theory. It can also observed that all experimental curves fall below the theoretically predicted curves, which means that at given flow rate, a higher pressure drop required to force the liquid to flow through those microchannels than the predictions of the conventional laminar flow theory.

We compare our results with Wilding et al. [8] who has microchannels with triangular cross-section with dimensions of 80x20 μm2 (WxH) and microchannel length of 11. 7 mm and found a good agreements.

The same agreements we get from the literature review done by G. Hetsroni [22], The behavior of the flow in microchannels, at least down to 50 μm diameter, shows no differences with macro-scale flow. The relation of hydraulic diameter to channel length and the Reynolds number are important factors that determine the effect of the viscous energy dissipation on flow parameters.

Microchannel cross sections

We check the dependence of the flow rate as a function of the pressure drop relationship to different cross sections, so microchannels with trapezoid cross section have hydraulic diameters of 57 μm and 29.1μm and microchannel with semi-circular cross section has hydraulic diameter of 48.8 μm. As shown in Figure 22and Figure 23 respectively, where as, the fluid that used in the experimental was distilled water and the Microchannels length is 11 mm.

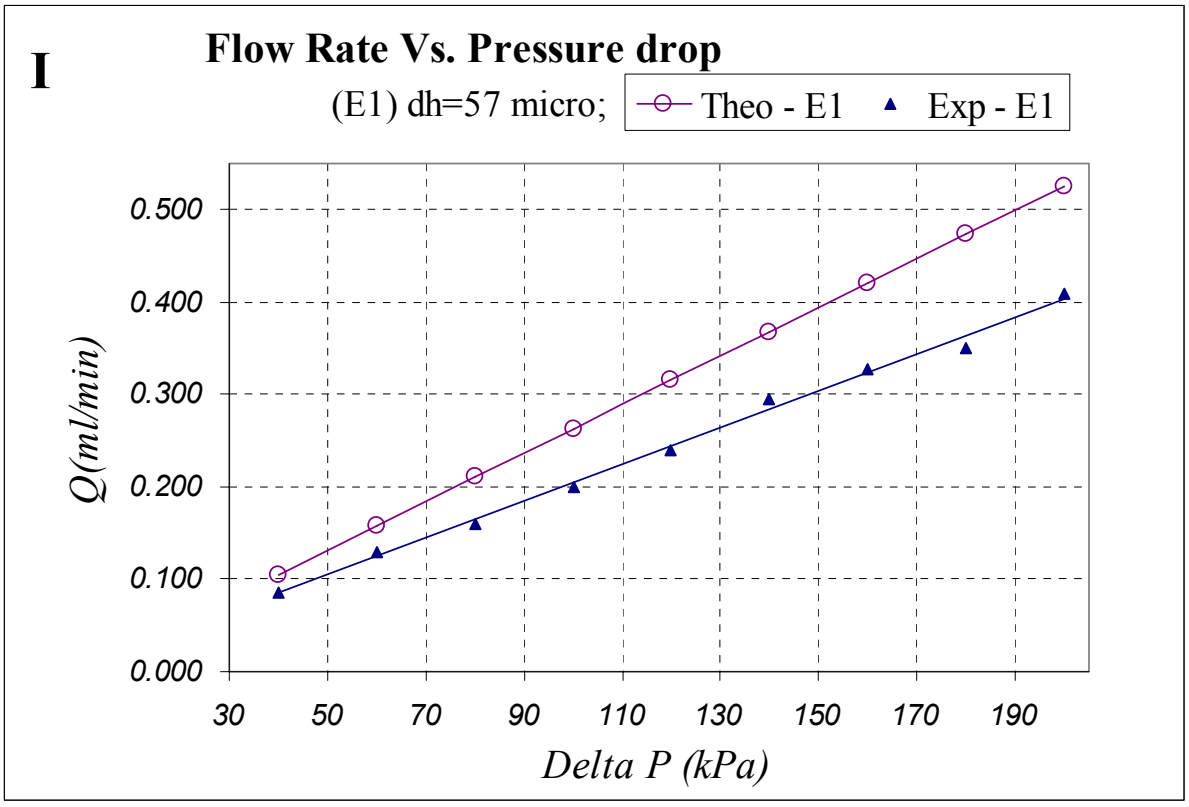

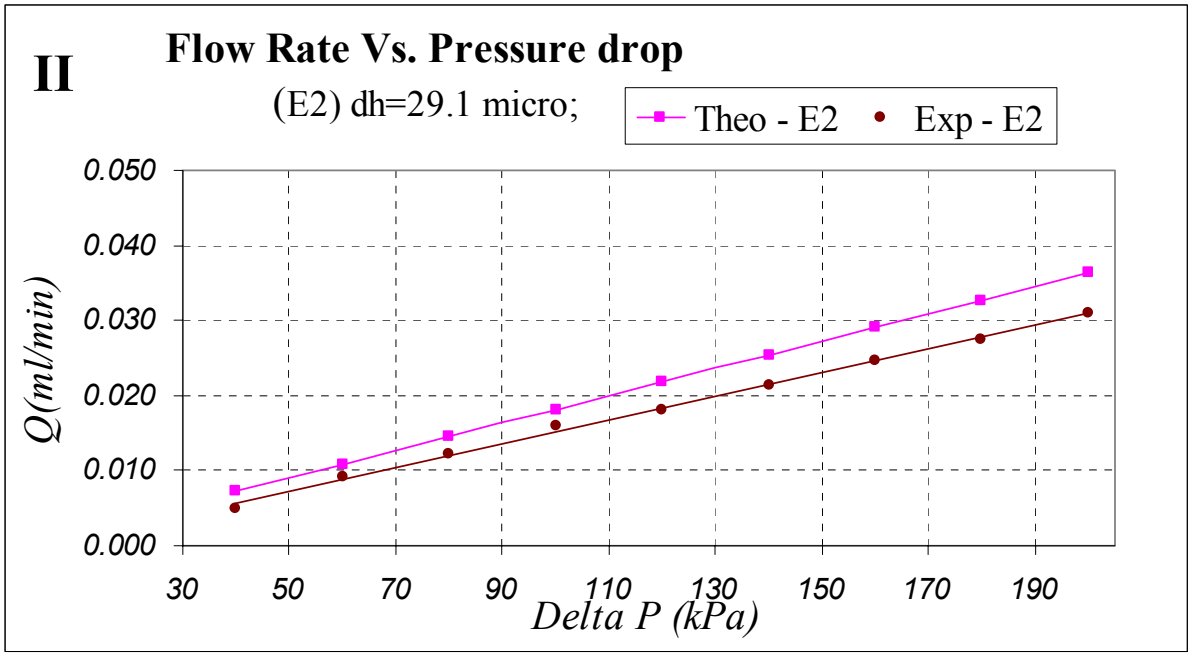

Figure 22: A Comparison of the measured data of flow rate vs. Pressure drop with the prediction of conventional laminar flow theory. Distilled water Flow in Trapezoid Cross-Section Microchannel with the Hydraulic diameters, I (E1) dh=57 μm; II (E2) dh=29.1 μm;

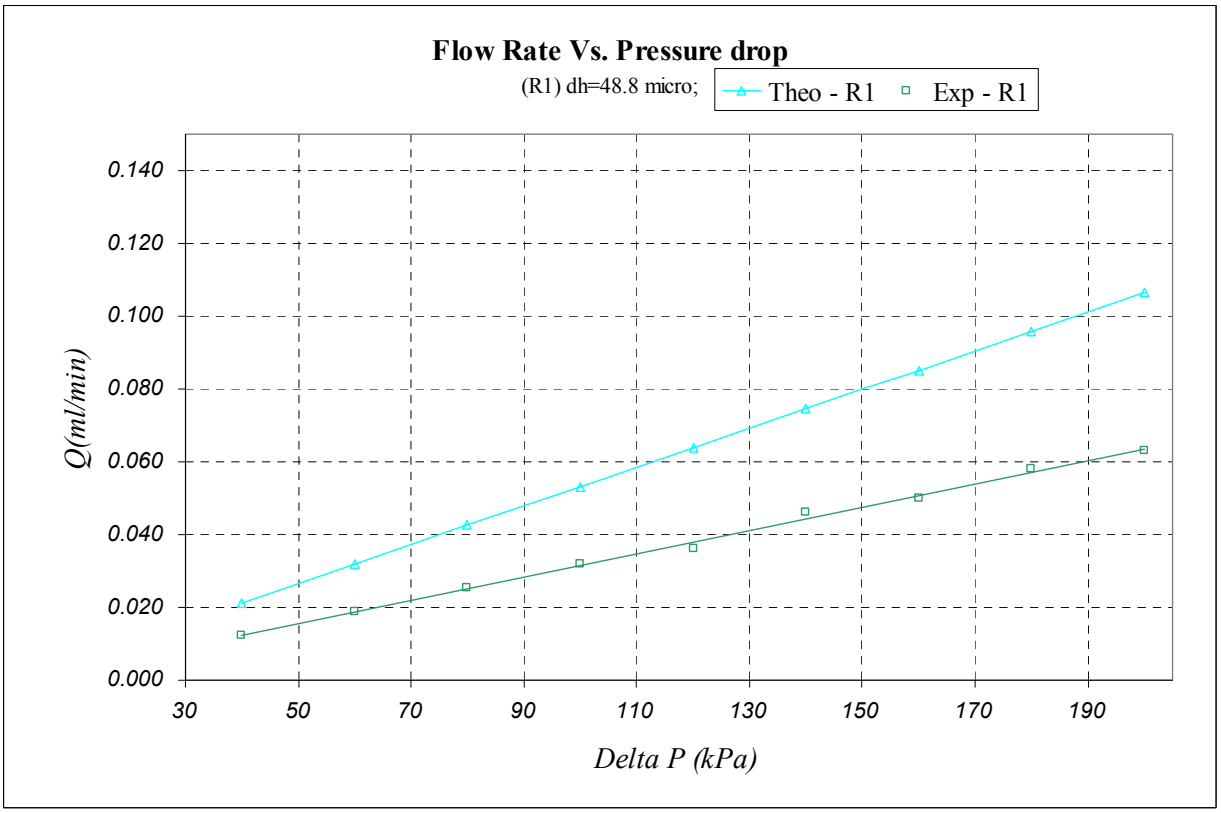

Figure 23: A Comparison of the measured data of flow rate vs. Pressure drop with the prediction of conventional laminar flow theory. Distilled water Flow in Semi-circular Cross-Section loped microchannel with the Hydraulic diameters, (R1) dh=48.8 μm;

A comparison is made between the experimental data obtained for Microchannels had triangular, trapezoidal and Semi-circular cross-sections, with hydraulic diameters ranging from 16.55 to 49.13 μm for triangular, 29,1 to 57 μm for trapezoidal and 48.8 μm for Semi-circular. The calculation flow based on conventional fluid mechanics.

The calculation essentially describes the relationship of flow rate to pressure.

Figures 21,22 and 23 indicate that, for Microchannels of dimensions considered, the calculation in this study based on the conventional fluid mechanics, can adequately predict the resulting flow chrematistics of the triangular, trapezoidal and Semi-circular cross-sections Microchannels.

It should be noted that the experimental curves are all linear as required by conventional laminar flow theory. It can also observed that all experimental curves fall below the theoretically predicted curves, which means that at given flow rate, a higher pressure drop required to force the liquid to flow through those microchannels than the predictions of the conventional laminar flow theory.

We have seen that no different in the behavior between triangular cross section to trapezoid and semi-circular cross sections, that means the microchannel cross section shape do not effect the flow behavior.

6.2.2 Pressure Gradient Vs. Reynolds Number

The measured pressure gradient $\frac{dp}{dx}$ is plotted in Figure 24 as a function of the experimentally determined Reynolds number, in triangular cross-section microchannel with the hydraulic diameters range from 16.55 μm to 49.13μm. Where as, the fluid was distilled water.

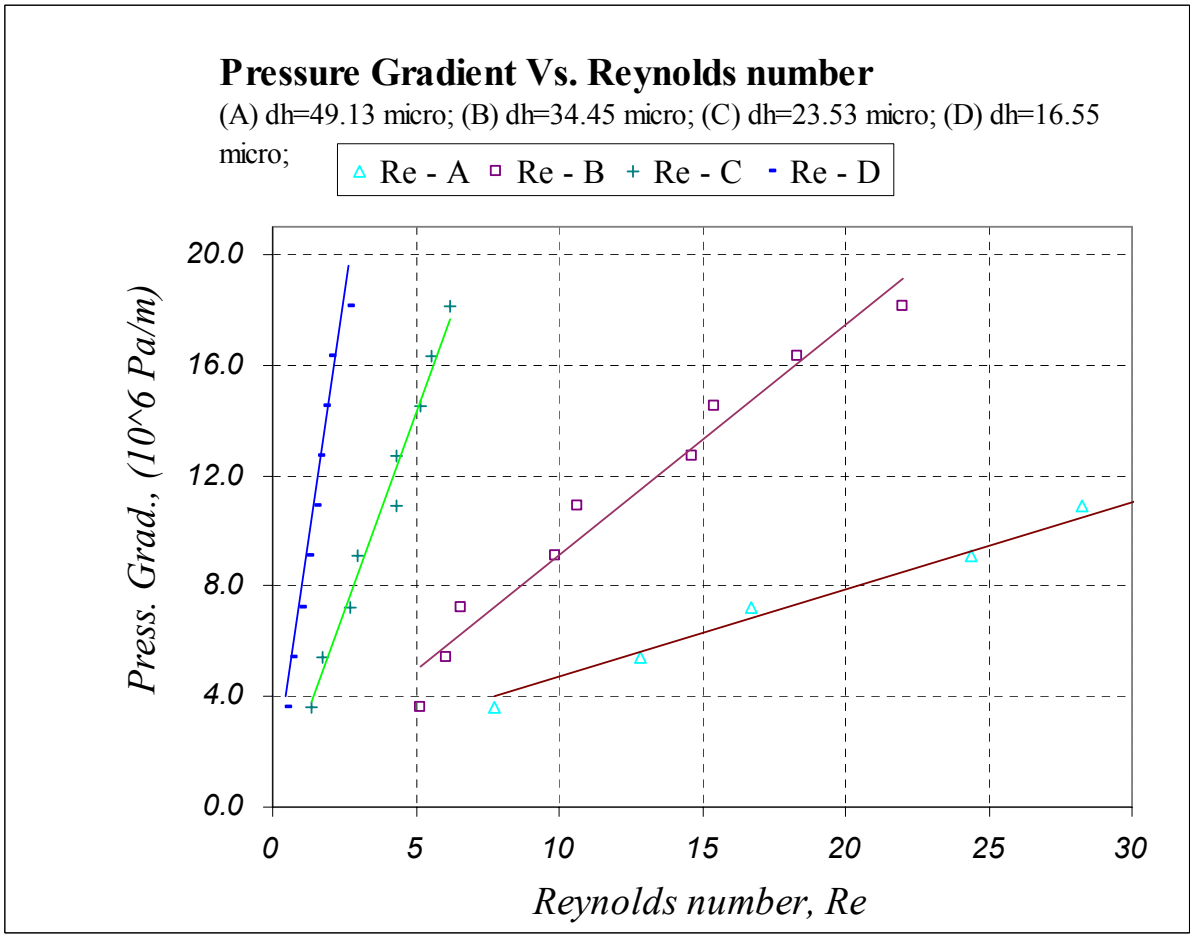

Figure 24: A comparison of the measured data of Pressure gradient vs. Reynolds number. Distilled water Flow in Triangular Cross-Section Microchannel with the Hydraulic diameters, (A) dh=49.13 μm; (B) dh=34.45 μm;(C) dh=23.53 μm; (D) dh=16.55 μm;

We investigate the microchannel size, as shown in Figure 24,the experimental $\frac{dp}{dx}$ - Re relationships are essentially linear as well. However, as the *Dh (*Hydraulic diameters) that represents the microchannels size increases the slopes of these experimental curves start to decrease.

We check the dependence of the $\frac{dp}{dx}$ - Re relationship to different cross sections, so microchannels with trapezoid cross section have hydraulic diameters 57 μm and 29.1μm. As shown in Figure 25,where as, the fluid was distilled water.

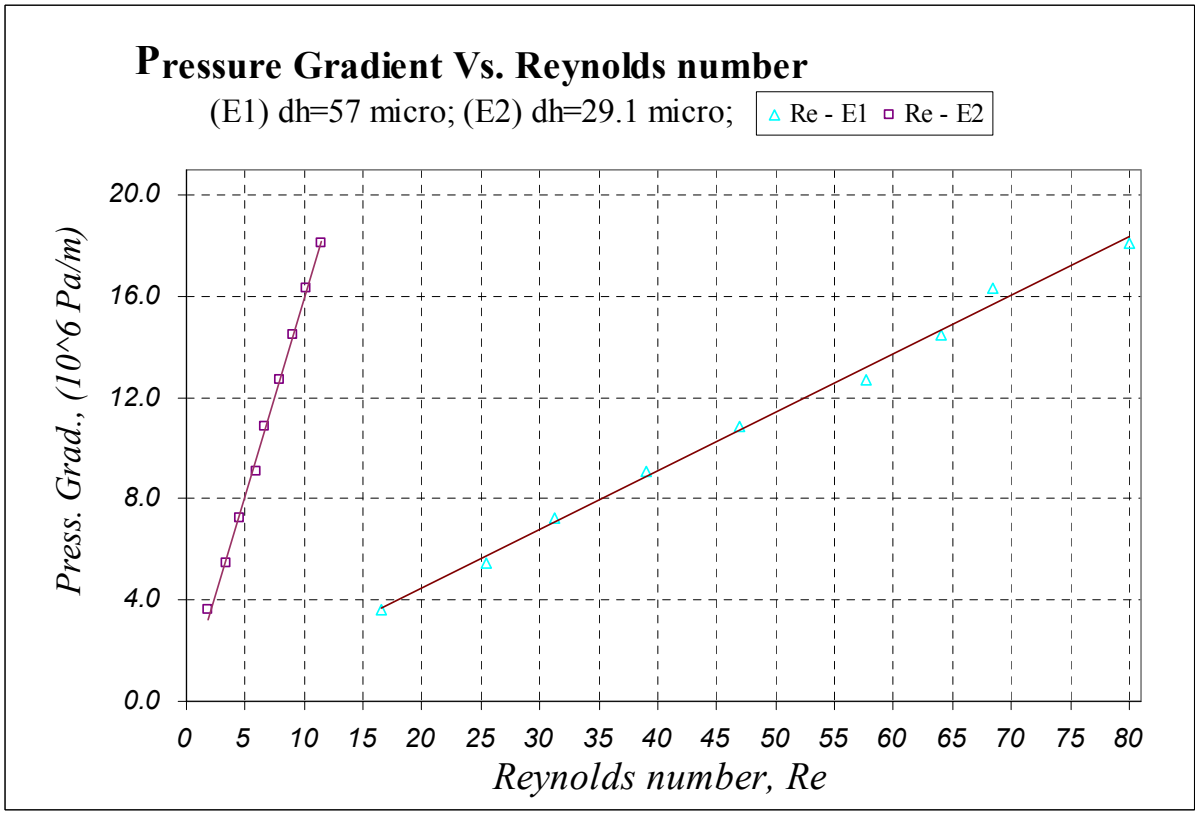

Figure 25: A comparison of the measured data of Pressure gradient vs. Reynolds number. Distilled water Flow in Trapezoid Cross-Section Microchannel with the Hydraulic diameters, (E1) dh=57 μm;(E2) dh=29.1 μm;

The experimental $\frac{dp}{dx}$ - *Re* relationships are essentially linear as well. However, as the *Dh* *(*Hydraulic diameters) that represents the microchannels size increases the slopes of these experimental curves start to decrease.

Which is the same behavior in triangular cross section, that means the cross section shape has not effect.

6.3 Comparing various fluids

We investigate the flow of various fluids Distilled water, Isopropanol, Ethanol and Glycerin in straight microchannel with Triangular Cross-Section 95 μm wide x 67 μm deep. The results obtained from 11 mm length Microchannels. The results of the measurements are present in Figure 26, the flow rate as a function of the pressure drop.

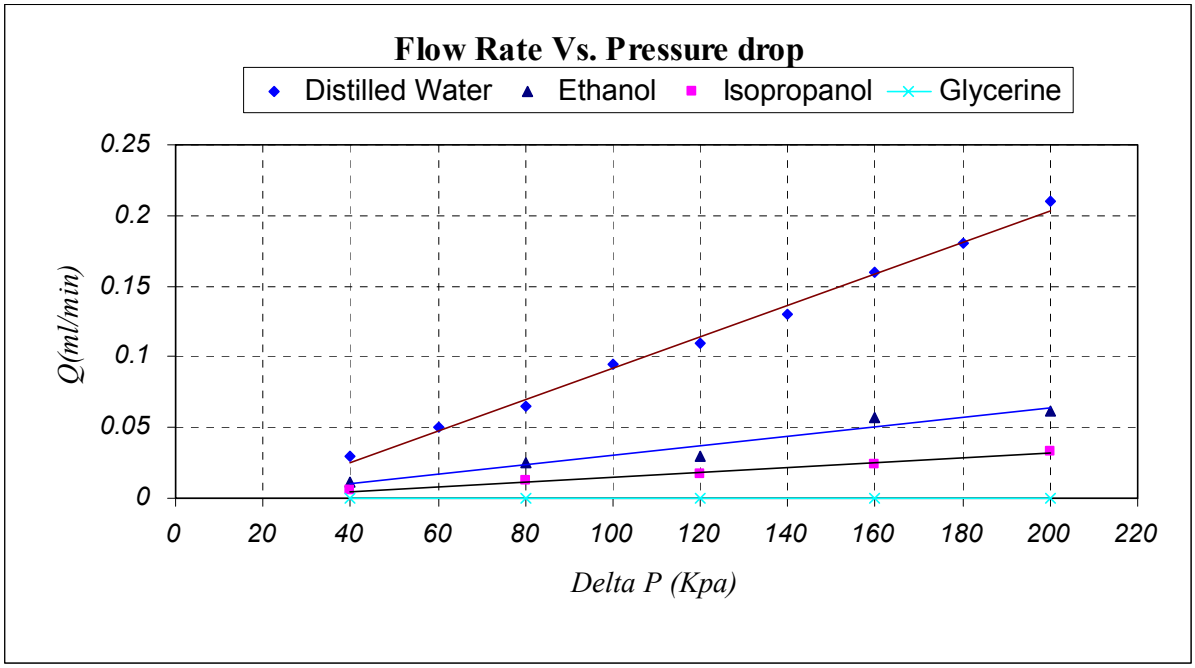

Figure 26: A Comparison of the measured data of flow rate vs. Pressure drop, different fluids flow in Triangular Cross-Section Microchannel 95 μm wide x 67 μm deep, with the Hydraulic diameter, dh=48.8 μm;

As shown in Figure 26, the experimental curves are all linear and all the fluid behavior linear. We compare our results with Wilding et al. [8] who analyzed flow of water and various fluids (Isopropanol, saline, Glycerin, serum, plasma, and whole blood) in glass-capped silicon microchannels and found that the behavior of the fluid in our experimental similar to their results on the same fluids.

6.4 Improvements to Microchannel System

There are a few opportunities for improvement of this microchannel in the areas of sealing and interfacing to macro world. Sealing problems encountered in the current design could possibly be prevented in two ways. Also to find the way of assembly gives the possibility of replacing the module easily.

The first is an alternative bonding method is anodic bonding, to be used instead of gluing techniques of the glass/silicon. Anodic bonding consists of placing a 500µm pyrex 7740 glass wafer (Corning, Corning, New York) over the silicon wafer and applying a voltage of 200-1000V at a temperature between 180°C and 500°C across the assembly

And this improvement has been done in advance stage of the research. In addition to providing a better sealing method, anodic boding would also provide a cleaned cross section of the microchannel from the gluing techniques that the glue get inside the microchannel which cause narrowness.

Another design modification to improve sealing is to replace the glue techniques of the module to the base adapter with a transparent plate, four bolts and two o-rings in the in/out ports of the module to the base adapter as shown in Figure 27. The plate would provide equal pressure on all sides of the microchannel module and tightening with a torque wrench would offer repeatable pressure acquisition.

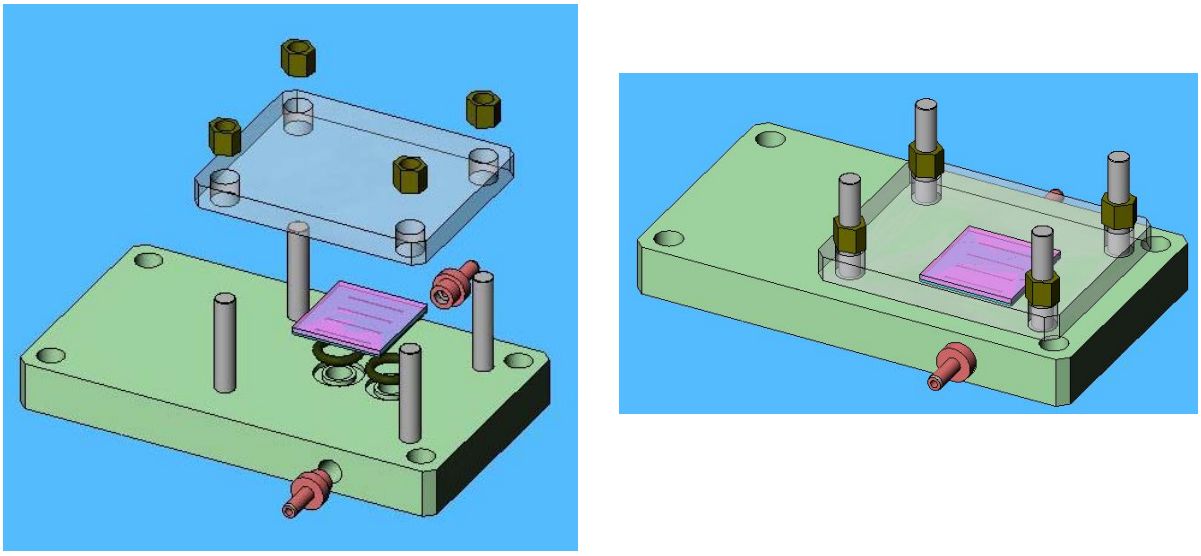

Figure 27: Schematic of improved Microchannels assembly.

Redesign the in/out ports of the assembly to be in the base adapter sides instead on the bottom, and instead to be glued the in/out adapters, they will be threaded in the base adapter, these improvements will offer flexibility of the attachment of the assembly, indeed to this improvement it used to release bubbles from the system as much close to the module.
So the new assembly is shown in Figure 27and the parts of this package were the new aluminum base adapter, the module itself, a transparent plastic plate 40 mm x 50 mm x 5 mm thick, four bolts, two o-rings in the in/out ports of the module to the base adapter and two adapters for in /out ports of the base adapter.
The base adapter is an aluminum rectangle that is 90 mm x 50 mm x 10 mm thick. To create the input and output ports in the base adapter, 1.5 mm diameter holes were drilled into 6mm opposite sides of the base adapter. These holes stop directly under the location where the fluid ports of the module will lie. Holes 5 mm in diameter were then drilled sides of the base adapter to meet the 1.5 mm diameter holes, with thread of M5 at the end. A 6.5-9 mm diameter slot with 1.5 depth was then milled over the 1.5 mm diameter ports to create pockets where the o-rings will sit. These holes complete the fluid pathway in the base adapter. A dimensional drawing of the base adapter is shown in Appendix B.
After the o-rings, module, and transparent plastic plate placed, the four bolts closed directly over the transparent plastic plate to engage the o-rings and create a sealed fluid circuit. After the seal is created, silicon tubing connected to the two adapters on the in /out ports of the base adapter. Such a packaging assembly allows modules to be changed easily with a ready fluid connection. The assembly is then ready to be placed on the experimental setup.

Figure 28: Pictures of the prototype of the improved microchannels assembly

7 Conclusions and Future Work

7.1 Conclusions

In our instigation we based on an experimental work, the main goal of this project examined a Lap-Biochip based microchannels that was designed and fabricated using microfabrication techniques, to investigate the microcirculatory.

Using microfabrication techniques, sufficient dimensional and geometric control was achieved. The silicon etching process developed allowed fabrication of a network of microchannels for the study of microcirculation. Using this process, microchannels that provide an in vitro method to isolate the varying microvessel size and geometries.

The theoretical curves of the flow rate as function of the pressure drop are all linear also the experimental as well, as it required by conventional laminar flow theory.

All experimental curves fall below theoretically predicted curves, which means that at given flow rate, a higher-pressure drop required to force the liquid to flow through those microchannels than the predictions of the conventional laminar flow theory.

The measured higher-pressure drop maybe be due to the effect of the surface roughness of the microchannels, or maybe be due to the pressure loss in the entrance in / out of the microchannels.

While the results in this study conform to macro scale laws, it is still an important result. It provides a basis from which future work can be undertaken in order to precisely predict where the result moves away from that which can be accurately estimated using conventional macro scale laws

Micro-fluidic systems are inherently low Reynolds number; it was found that the liquid Reynolds number is dramatically affected by the channel size reduction.

The comparison of the flow of various fluids Isopropanol, Ethanol and Glycerin with Distilled water in straight microchannel was behave linear as expected in conventional flow.

As described in the beginning of this work, the research aim is to investigate the microcirculatory and blood flow thru microchannels but because time conditions the work stop at this stage without get to final goal but it provides the a proof base to continue to final goal. The system is ready to investigate the microcirculatory and blood flow, more then it provides a basis form which future work can be undertaken in order to continue.

7.2 Future Work

Additional experiments needed to check how the entrance and outlet area affect the flow behavior in microchannels.
In additional, our system ready to be coated with organic materials and performed
Several experiments, and study the flow in branching microchannels
The microchannel system developed will be used to study cell deformation and motility as affected by protein expression in the growth and spread of colon cancer.
In addition, the system can also be used to begin a study on the flow through porous media.
To isolate microvessel surface roughness and test wall coating, to design another set of microchannels with a bumpy contour modeled after endothelial cells applied to the microchannel walls. Check the effect of the endothelial coating on the flow in branching microchannels.
To develop a “Lap-on-chip” LOC used in blood analysis for several diseases.

8 References

8.1 Articles

1. R. Willem Tjerkstra, Meint de Bore, 1997 “Etching Technology For Microchannels”, IEEE, MESA Research Institute, University of Twente, pp. 147-152.
2. Johansson S., Gustavsson K. and Schweitz J., 1998 ” Strength Evaluation Field-assised Bond Seals between Silicon and Pyrex Glass”, Sensors and materials, vol. 1,pp.143-151.
3. Flockhart S. M., Dhariwal R. S., 1998,”Experimantal and Numerical Investigation Into the Flow Characteristics of Channels Etched in <100> Silicon”, Journal of Fluids Engineering, Vol. 120, pp. 291-295.
4. Harley J., Bau H., 1989,”Fluid Flow in Micron and Submicron Size Channels”, Proceedings IEEE MEMS, pp. 25-28.
5. Pfahler J., Harley J., Bau H. and Zemel J., 1991,”Gas and Liquid Flow in Small Channels”, Micromechanical Sensors Actuators and Systems, DSC- Vol. 35, pp. 49-59.
6. Sutton N., Tracey M. N. and Johnston I. D., 1997,”A Novel Instrument for Studying the Flow Behaviour of Erythrocytes through Microchannels Simulating Human Blood Capillaries”, Microvascular Research, Vol. 53, pp. 272-281.
7. Weilin Qu., Mohiuddin Mala Gh., Dongqing Li., 2000,”Pressure-driven Water Flows in Trapezoidal Silicon Microchannels”, International Journal of Heat Transfer, Vol. 43, pp. 353-364.
8. Wilding P., Pfahler J., Bau H., Zemel J., Kricka J., 1994,” Manipulation and Flow of Biological fluids in Straight Channels Micromachined in Silicon ”, Clinical Chemistry, Vol. 40, No. 1, pp. 49-59.
9. Gravesen P., Branebjerg J., Jensen O., 1993,”Microfluidics-a review”, J. Micromech. Microeng. , Vol. 3, pp. 168-182.
10. Koo J., Kleinstreuer C., 2003,”Liquid Flow in Microchannels: Experimental Observations and Computational Analyses of Microfluidics Effects ”, J. Micromech. Microeng. , Vol. 13, pp. 568-579.
11. Paul L. La Celle, 1986,” Alterations by Leukocytes of Erythrocyte Flow in Microchannels”, Blood Cells, Vol. 12, pp. 179-189.
12. Papautsky I., Brazzle J., Ameel T. and Frazier A B., 1998,” Microchannel Fluid Behavior Using Micropolar Fluid Theory”, Sensors Actuators, Vol. 73, pp.101-108.

13. Tsukada K., Sekizuke E., Oshio C. and Minamitani H., 2001,"Direct measurement of Erythrocyte Deformability in Diabetes Mellitus with a Transparent Microchannel Capillary Model and High-Speed Video Camera System", Microvascular Research, Vol. 61, pp. 231-239.
14. Secomb, T.W., Skalak, R., Ozkaya, N. and Gross, J.F., 1986," Flow of Axisymmetric Red Blood Cells in Narrow Capillaries", J. Fluid Mech., Vol.163, pp.405-423.
15. Cokelet G.R., Soave R., Pugh G. and Rathbun L., 1993,"Fabrication of in vitro Microvascular Blood Flow Systems by Photolithography", Microvascular Research, Vol. 46, pp. 394-400.
16. Trebotich D., Chang W. and Liepmann D., 2001," Modeling of Blood Flow in Simple Microchannel", Modeling and Simulation of Microsystems 2001,pp.218-222.
17. Chang W., Trebotich D., Lee L. and Liepmann D., 2000," Blood Flow in Simple Microchannel", Microtechnologies in Medicine & Biology 2000,pp.1-5.
18. Tracey, M.C., Greenaway, R.S., Das, A., Kaye, P.H., and Barnes, A.J., 1995," A Silicon Micromachined Device for Use in Blood Cell Deformability Studies", IEEE Transactions on Biomedical Engineering, Vol. 42, pp. 751-761.
19. Jiang X. N., Zhou, Z. Y., Yao, J., Li, Y., and Ye, X. Y., 1995, "Micro-fluid flow in microchannel," Transducers '95, Stockholm, Sweden, June 25-29, pp. 317-320.
20. Gale, B. K., 2000, "Scaling effects in a microfabricated electric field flow fractionation system with integrated detector," Ph.D. thesis, University of Utah, Salt Lake City.
21. Kikuchi Y, Sate K, Ohki H and Kaneko T., 1992, "Optically accessible microchannels formed in a single-crystal silicon substrate for studies of blood Rheology", Microvascular Research, Vol.44, pp. 226-240.
22. G. Hetsroni, A. Mosyak, E. Pogrebnyak and L.P. Yarin, 2005, "Fluid flow in microchannels", International Journal of Heat and Mass Transfer, Vol. 48, pp.1982–1998.

8.2 Books

23. Frank M. White, Fluid Mechanics, 4th ed., McGraw-Hill, New York, 1999.
24. Fung, Y.C., Biomechanics: Mechanical Properties of Living Tissues. 2 ed. 1993, New York, New York: Springer.
25. Ronald L. Fournier, Basic Transport Phenomena in Bio-Medical Engineering, Taylor & Francis, Philadelphia, 1998.

26. Michele C., Michael W.and Tom R., Nanoscale Fluid Dynamics in Physiological Processes, WIT Press, UK, 1999.
27. Daniel J. and Joseph D., Biomechanics Principles and Applications, CRC Press LLC, Boca Raton, 2000.
28. Richard S. and Shu C., Handbook of Bioengineering, McGraw-Hill, New York, 1987.
29. Mohamed Gad-el-Hak, The MEMS Handbook "Liquid Flows in Microchannels", CRC Press LLC, Boca Raton, 2002.
30. Shah R. K. and London A. L., Laminar Flow Forced Convection in Ducts, Academic Press, New York, 1978.
31. Michel Y. J. and Colin G.C., Biological Flows, Plenum Press, New York and London, 1995.

8.3 Websites

1. http://www.pennhealth.com/health_info/bloodless/images/19432.jpg.
2. http://whyfiles.org/090doping_sport/images/redblood.jpg.

9 Appendixes

9.1 APPENDIX A - Resistance to Flow

TABLE 6.2 Resistance to Flow in Fully Developed Flow Through Straight Microchannels of Various Cross-Sectional Geometries

Cross Section	$f\,Re$	u_{max}/u_B
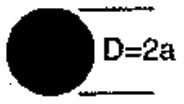	64	2.000
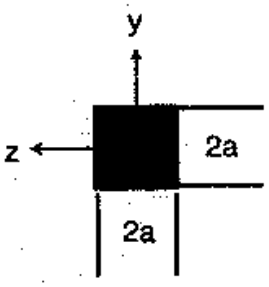	56.92	2.0962
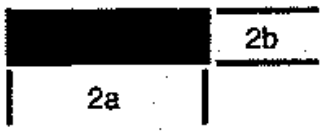	$96[1 - 1.3553\alpha + 1.9467\alpha^2 - 1.7012\alpha^3 + 0.9564\alpha^4 - 0.2537\alpha^5]$	—
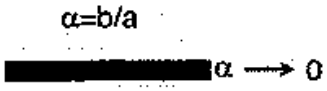	96	1.5000
	60	—
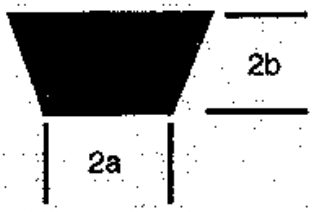	2b/2a 4.000 55.66 2.000 55.22 1.000 56.60 0.500 62.77 0.250 72.20	 2.181 2.162 2.119 1.969 1.766
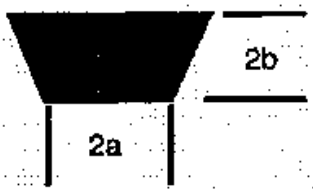	1.000 56.15	2.137

Source: Data from Shah, R.K., and London, A.L. (1978) *Advances in Heat Transfer*, Suppl. 1, Academic Press, New York.

9.2 APPENDIX B- Base Adapter

- Base Adapter manufacture drawing

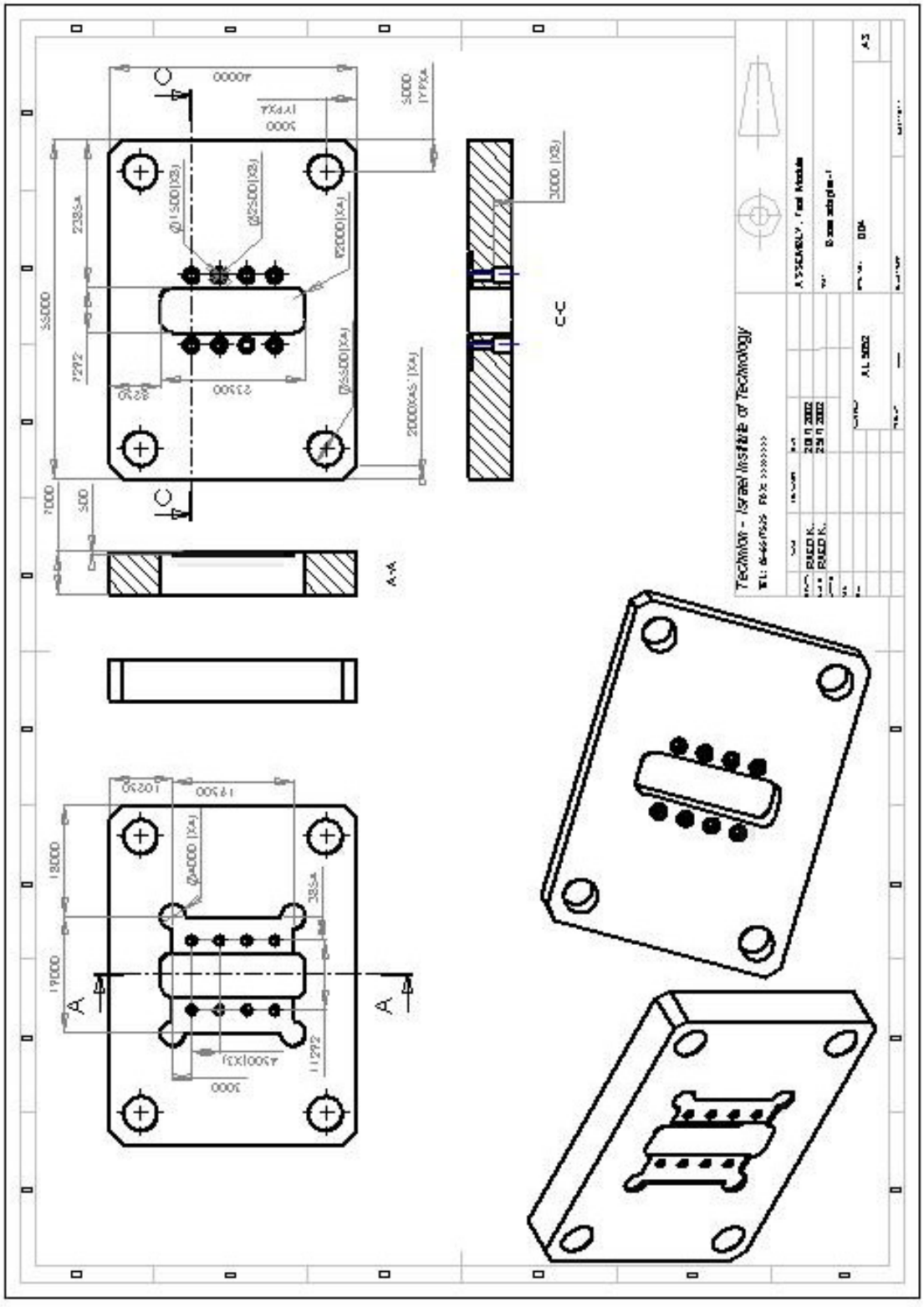

- Base Adapter manufacture drawing, after improvements